

Failure Prediction of NiMH Batteries



Filip Dahlberg
Markus Hägnfelt

Division of Industrial Electrical Engineering and Automation
Faculty of Engineering, Lund University

FACULTY OF ENGINEERING LTH AT
LUND UNIVERSITY

Failure Prediction of NiMH Batteries

Students:

Filip DAHLBERG
Markus HÄGNEFELT

Company supervisor:

Roger DREYER

Supervisor:

Gunnar LINDSTEDT

Examiner:

Johan BJÖRNSTEDT

June 21, 2018

Abstract

This master thesis has been carried out to investigate the possibility to predict battery failure of Nickel-Metal Hydride (NiMH) batteries. Assa Abloy use these batteries as a back-up in their door solution systems in case there is a power loss. The main function is to be able to open doors that are part of an emergency exit route. Thus, approximately 200 battery packs were used to collect data regarding mainly their internal resistance, capacity and age counted from production date. These parameters were then mapped to how many consecutive door openings they could perform at different temperatures before failure. The study showed that the internal resistance of the battery has a great impact on its performance. The temperature also has a big effect because the internal resistance varies with temperature. At a late stage of the master thesis, it was seen that the open circuit voltage during charge was affected by the temperature. However, more investigation regarding this needs to be done. Furthermore, the capacity does not seem to have a notable impact and neither does the age. The key to predict battery failure is to have knowledge regarding how the internal resistance changes over time as well as how it changes with temperature. Some insight regarding this has been discovered during the study but further investigation needs to be done.

Preface

This master thesis regarding failure prediction of Nickel-Metal Hydride batteries has been written to fulfill the graduation requirements of the Mechanical Engineering program at the Faculty of Engineering LTH at Lund University. The project has been carried out from September -17 to January -18 upon request from the *R&D* department at Assa Abloy, Landskrona.

First of all we would like to thank Roger Dreyer for giving us the opportunity to write our master thesis at the *R&D* department at Assa Abloy. Roger was also our supervisor who always gave us our full attention when needed. More over, we would like to thank the co-workers at the *R&D* department who shared their experience and knowledge when questions occurred.

We would also like to thank our supervisor and examiner at the university, Gunnar Lindstedt and Johan Björnstedt, who has helped us throughout the project when it was needed.

At last, we would also like to mention that the parameters α_1 , α_2 and α_3 are three different constants that have been used to censor some data throughout the report. α_1 has been used for resistances, α_2 for voltages and α_3 for currents.

Definitions

α_1 Constant used to censor resistance values.

α_2 Constant used to censor voltage values.

α_3 Constant used to censor current values.

AA-battery Standardized battery format, 49.2-50.5 mm length and 13.5-14.5 mm width.

Battery pack The battery mounted in an Assa Abloy slider door consist of two battery packs, where a battery pack is 10 AA-batteries connected in series.

Battery pair A battery pair consist of two battery pack connected in series.

Self discharge A battery's decline in voltage which takes place after charging is completed and charging device is turned off.

Slider door Slider door defines the product family where the door slides in the direction of the wall during an opening-procedure.

State of health a battery's state of health is a figure that tells a battery's condition. It is expressed as the ratio of a battery's actual capacity and its rated capacity. The state of health deteriorates when a battery ages and is under use.

Trickle charging trickle charging is the method employed to keep the Assa Abloy's batteries in fully charged condition. This is done by charging the battery pack's with 55 mA. [2].

Acronyms

DPH Dual Pulse High voltage point. This is the voltage value retrieved at node 2 on measurement board, see figure 13.

DPL Dual Pulse Low voltage point. This is the voltage value retrieved at node 2 on measurement board, see figure 13.

NiMH Nickel-Metal Hydride.

SCSDP Slow Charge and Self Discharge Phase.

SDP Self Discharge Phase.

Contents

1	Introduction	7
1.1	Background	7
1.2	The objective	7
2	Theory	9
2.1	NiMH battery	9
2.2	Chemical reaction in NiMH battery	9
2.3	Assa Abloy's battery pack	10
2.4	Capacity	10
2.4.1	Measure capacity	11
2.4.2	Capacity Indicator	11
2.5	Internal Resistance	13
2.5.1	Dual Pulse Method	14
2.5.2	High Current Method	14
2.6	Charge Characteristics of NiMH-battery	15
2.7	Discharge characteristics of NiMH-battery and its effect on capacity measurement	17
2.8	Self Discharge Characteristics	18
3	Methodology	20
3.1	Investigation	20
3.2	Acquisition of battery data	20
3.3	Battery performance	22
3.4	Design of hardware	23
3.4.1	Choice of microcontroller	23
3.4.2	Slow Charge and Self Discharge PCB	24
3.4.3	Measurements PCB	24
3.4.4	Capacity Measurement Board	26
3.4.5	Miscellaneous functions	27
3.5	Verification of circuit boards	28
3.5.1	Accuracy of internal resistance measurement	28
3.5.2	Accuracy of battery voltage measurement	29
3.6	Measurement Sequence	31
3.6.1	Fast charge using Assa Abloy's battery rack	31
3.6.2	Slow Charge and Self Discharge Phase	31
3.6.3	Measurements Phase	32

3.6.4	Capacity Measurement	32
3.7	Battery performance based on measured parameters	32
4	Results	34
4.1	Capacity	34
4.1.1	Self discharge's correlation to capacity	34
4.1.2	Capacity indicator's correlation to capacity	36
4.1.3	Capacity indicator's correlation to door openings	37
4.2	Age of battery counted from production date	38
4.3	Internal Resistance	39
4.4	Temperature	42
5	Discussion	46
5.1	The capacity's impact on battery performance	46
5.2	Capacity indicator's correlation to battery performance	46
5.3	The temperature's impact on the open circuit voltage	47
5.4	Conclusions	47
5.4.1	Internal Resistance's impact	47
5.4.2	Capacity's impact	48
5.4.3	Temperature's impact	48
5.4.4	Age's impact	48
5.4.5	Capacity Indicator's impact	48
5.4.6	Failure prediction - What is needed?	48
A	Verification data	51
A.1	Internal resistance measurement	51
A.2	Verify Measurements Board	54
A.3	Verify SCSD Board	56
A.4	Verify Capacity Measurement Board	58
A.5	Self discharge curves for all batteries	59

1 Introduction

As the global leader of door solutions, Assa Abloy consistently tries to find new methods to develop their products and make them more robust and safe. This master thesis has been carried out to investigate if there is a way to predict when the batteries in their slider doors needs to be replaced.

1.1 Background

In the slider doors of Assa Abloy, a backup battery-pack is installed as an alternative power supply in case there is a power outage from the electricity grid. The battery-pack's main function is to open the emergency exit doors during a power outage but can also be used to let non-emergency exit doors operate as normal during a power outage. Because it is such an important feature and regulated by law, Assa Abloy has to make sure that the battery-pack is in a good condition at all times. In order to do this, Assa's software makes a daily automatic test of their batteries. Should the battery-pack fail during the test, the door is set to a safe mode until it has been replaced. Unscheduled maintenance which this would result in should be avoided if possible and thus, this master thesis examines the possibility to predict battery failure.

1.2 The objective

Instead of changing batteries on a very short notice due to a failed test, Assa Abloy wants to be able to have detailed information of their batteries and predict their failure. As mentioned above, this master thesis is carried out to investigate if it is possible to predict the failure of the battery by measuring a number of key parameters. By measuring key parameters that have a correlation to a battery's performance, one will be able to tell the condition of the battery and hence give a prediction of how close the battery is to failure.

Assa Abloy defines battery failure in two ways; the battery voltage drops below a certain voltage level during an opening or the door opening procedure takes longer than five seconds to perform. A battery failure is most likely to occur during an opening procedure. Hence, a battery pack's ability to deliver power during an opening procedure is a core characteristic to be analyzed in this master thesis. Measurable factors that might have an

impact on the occurrence of a battery failure are presented as hypotheses. These hypotheses are developed in the perspective of what is defined as a battery failure which is mentioned above. In order to tell the correctness of the hypotheses, all measurable battery characteristics in the hypotheses; internal resistance, voltage drop after five seconds of load, capacity, time since manufacture date and temperature, will be compared with a battery's ability to open an automatic door.

1. The likelihood of battery failure is correlated to the internal resistance of a battery pack.
2. The likelihood of battery failure is correlated to the magnitude of a voltage drop occurring from current conducted from a battery during a five seconds period.
3. The likelihood of battery failure is correlated to the actual capacity expressed in mAh of a battery.
4. The likelihood of battery failure is correlated to the age of the battery, age of a battery is measured from manufacture date.
5. The likelihood of battery failure is correlated to the temperature of the battery when it supplies the power to perform an opening procedure.

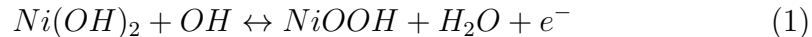
2 Theory

2.1 NiMH battery

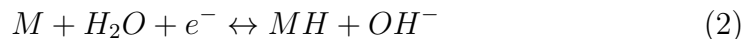
As for all batteries, the NiMH battery has one negative electrode, one positive electrode and one electrolyte. The positive electrode consists of Nickel Hydroxide (Ni(OH)_2), whereas the negative electrode consists of a Hydroxide absorbing alloy. The electrolyte is in most cases Potassium Hydroxide (KOH). Hydrogen is the active substance which stores the energy. The two electrodes are separated by a separator. The separator prevents short-circuit between the two electrodes while letting ions diffuse through which makes it possible for current to flow through the electrode layers. The separator is made of a synthetic material. A NiMH battery also contains a current collector which consists of a metal grid. The function of a current collector is to minimize internal resistance. [3]

2.2 Chemical reaction in NiMH battery

In the positive electrode, Nickel-hydroxide molecule reacts with hydroxide which produces an electron. This electron will travel through the electrical circuit and be absorbed by the alloy in the negative electrode. This process represents charging whereas the opposite reaction direction represents discharge. This can be seen in equation 1.



In the negative electrode, one electron and one hydrogen-ion is absorbed, see equation 2. This direction of equation 2 represents charging whereas the opposite direction represents discharge.



A combined reaction of the positive and negative electrode can be seen in equation 3, this is achieved by summing up equation 1 and 2. A graphical illustration of this can be seen in figure 1.



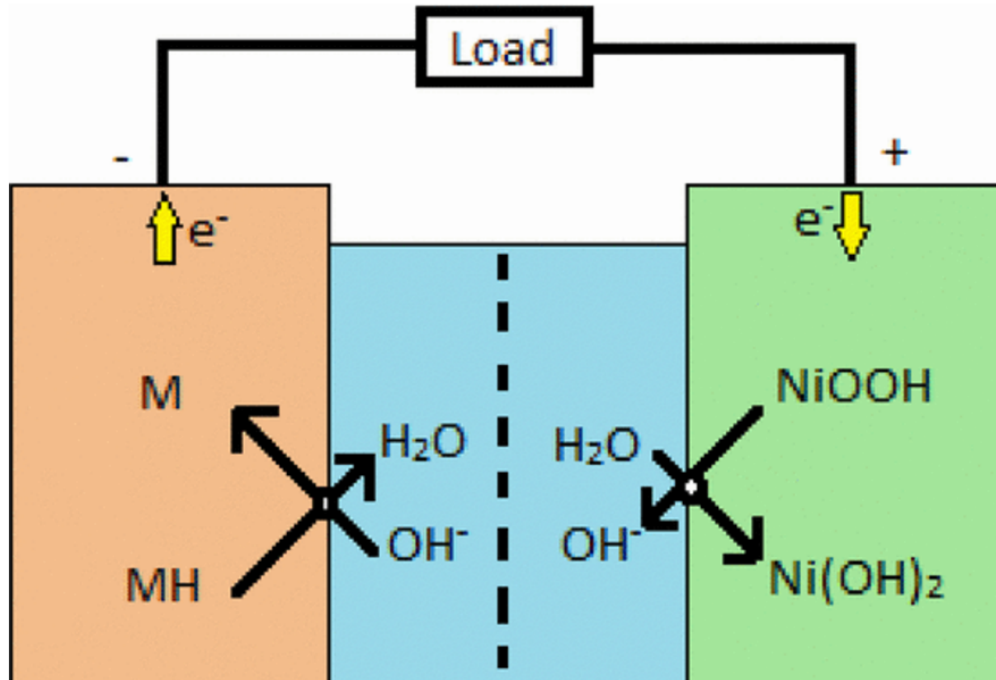


Figure 1: Chemical illustration of a NiMH battery's charge- and discharge characteristics.

2.3 Assa Abloy's battery pack

The battery-pack used in Assa Abloy's slider doors contains 10 AA-batteries connected in series. Connecting the batteries in series increases the voltage level by tenfold, from approximately 1.3V to 13V, while the capacity remains the same. In their slider doors, two battery-packs are connected in series to increase its power.

2.4 Capacity

The capacity of a battery is the amount of energy stored in it. It is measured in ampere hours (Ah).

2.4.1 Measure capacity

To measure the capacity of a battery, the amount of ampere hours can be calculated by drawing a current from the battery and consistently measure the current until the battery reaches the knee of discharge. Figure 2 shows the characteristics of discharging a battery, where the knee of discharge can be seen. The following equation can be used to calculate the capacity:

$$C = \int_0^T I dt \quad (4)$$

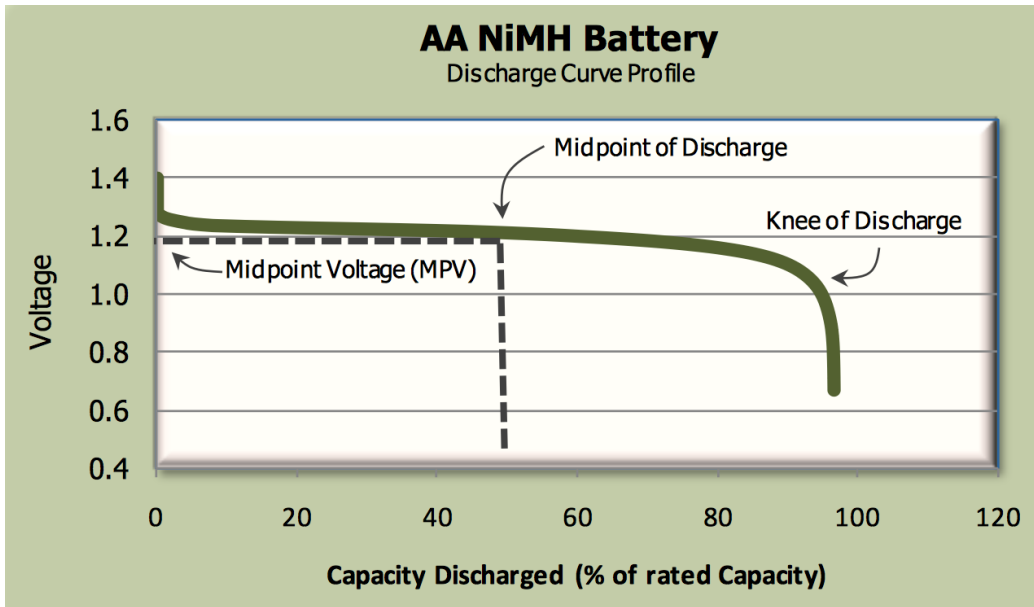


Figure 2: Knee of discharge. Figure taken from energizer.com

2.4.2 Capacity Indicator

As stated in the hypothesis, the magnitude of the voltage drop that occurs when a specific current is drawn from a battery during five seconds is correlating to the probability of battery failure, the battery model employed can be seen in figure 3. The reasoning to this hypothesis is as follows: the opening time for an automatic door depends on the voltage the battery can maintain during its opening procedure. Therefore it makes sense to measure

the voltage drop of the battery during the longest acceptable opening time; five seconds. This reasoning is valid since the work needed to open an automatic door can be seen as constant since the test will be performed on a worst case scenario door, i.e. all other automatic doors will request less work compared to the one that this test is performed on.

It should be noted that this method was implemented on request from Assa Abloy as a method to indicate a battery's capacity, hence the chosen method name "Capacity Indicator". The voltage drop for this method will be calculated as described in equation (5). At time $t = 0$ s, there will not be any current conducted, while during time $0 < t \leq 5$ s the current is conducted as shown in equation (7).

$$\text{Capacity indicator} = U_{\text{battery}}(t = 0) - U_{\text{battery}}(t = 5s) \text{ [V]} \quad (5)$$

$$I_{\text{battery}}(t = 0) = 0 \text{ [A]} \quad (6)$$

$$I_{\text{battery}}(0 < t \leq 5) = \frac{U_{\text{battery}}(t)}{R_{11}} \text{ [A]} \quad (7)$$

R_{11} can be seen in figure 13.

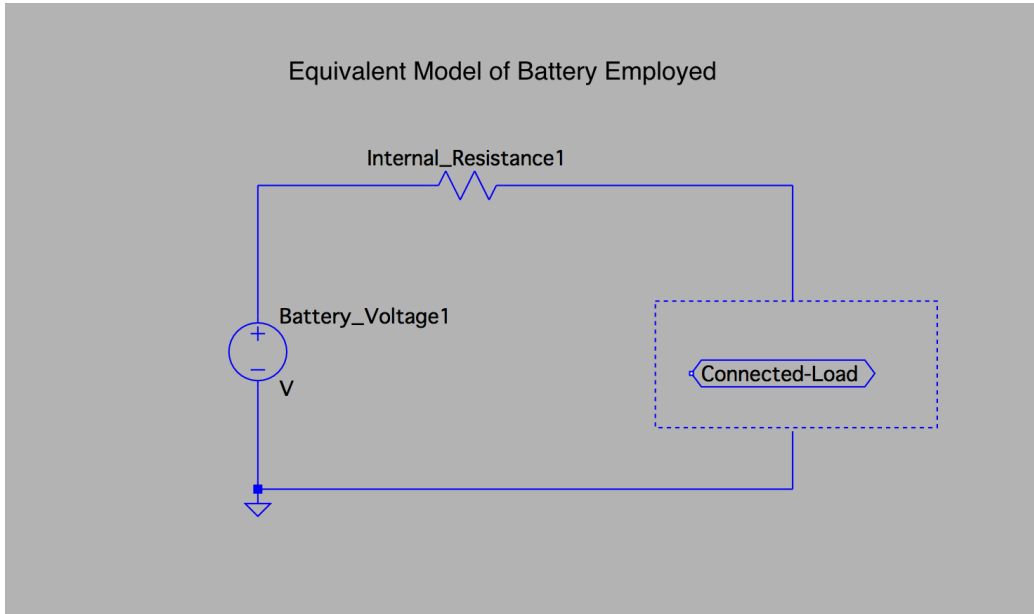


Figure 3: The battery model employed.

2.5 Internal Resistance

The internal resistance of a battery is the opposition to the flow of current within the battery. The internal resistance consists of the electronic resistance and the ionic resistance. The electronic resistance encompasses the individual resistivity of the materials used and how well they make contact to each other. The ionic resistance is dependent on electrochemical factors, such as the ion mobility, electrolyte conductivity and electrode surface area. A number of factors that affect the internal resistance of a battery are the age, the ambient temperature, charge and discharge cycles, the depth of discharge, the magnitude of the current drawn and the chemical composition of the battery [4]. Figure 4 shows how the internal resistance varies with temperature in a fresh Energizer E91 AA battery. The reason why the internal resistance increases as temperature drops is because the electrochemical reactions slow down and decrease the ion mobility in the electrolyte. To measure the internal resistance of a battery, [4] describes two methods.

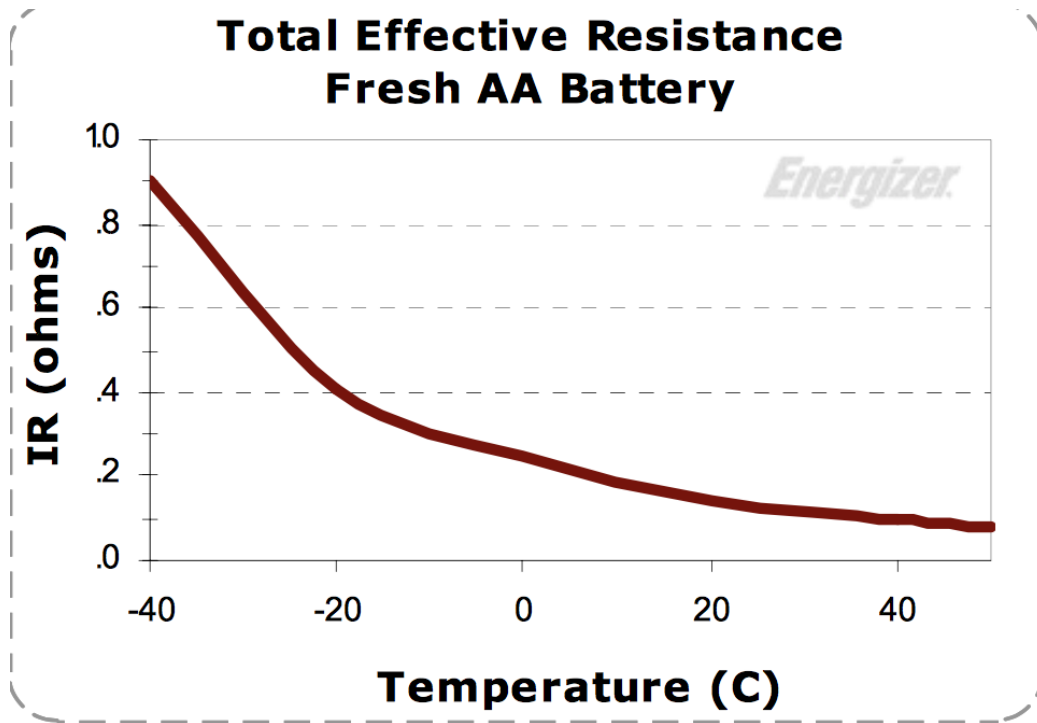


Figure 4: Internal resistance based on temperature. Figure taken from energizer.com.

2.5.1 Dual Pulse Method

The Dual Pulse Method is done by first drawing a low stabilizing current, I_L , and at the same time measure the voltage of the battery, U_L , followed by increasing the current to I_H and once again measure the voltage, U_H . L and H are indexes for low and high. With these values, the internal resistance can be calculated based on Ohm's law:

$$R_{internal} = (U_L - U_H)/(I_H - I_L) \quad (8)$$

Figure 5 shows an example of this method.

2.5.2 High Current Method

To measure the internal resistance with the High Current Method, the battery is loaded with a 0.01 ohm resistor for 0.2 seconds. The current drawn

can be calculated using the closed circuit voltage.

$$I = U_{CCV}/0.01 \quad (9)$$

The internal resistance can then be calculated using the open circuit voltage and the current calculated in the equation above.

$$R_{internal} = U_{OCV}/I \quad (10)$$

Using this method, it can be difficult to measure the closed circuit voltage when the high current is drawn since it is drawn during a very short period.

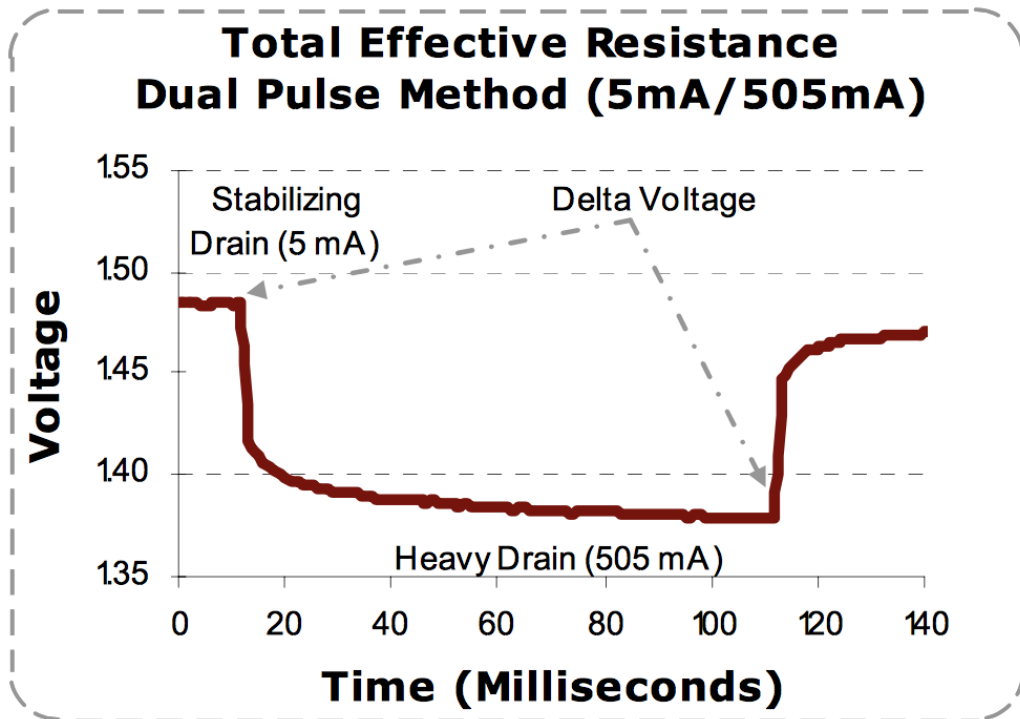


Figure 5: Dual Pulse Method. Figure taken from energizer.com.

2.6 Charge Characteristics of NiMH-battery

Using correct charging techniques of batteries is very important to reach a satisfying performance. Both under-charging, which is when the batteries are not fully charged and over-charging should be avoided if possible. Under-charging the battery can result in low service and over-charging can cause

loss of life cycle. To determine when the battery has reached full charge, key parameters to look at is the temperature of the battery and if the battery has reached its voltage peak. The temperature will drastically increase once it reaches over-charge because the majority of the electrical energy input to the battery will convert to heat instead. Figure 6 shows the charging characteristics of a battery charged at a rate of 1C. C is the standard battery rating which is the capacity of a fully charged battery. Using a charge rate of 1C would thus theoretically fully charge a battery in one hour. By studying the figure, it is seen that the pressure and temperature increases when the battery reaches full charge. It can also be seen that the voltage reaches a peak, after which it starts to decrease.

[2] states that a moderate rate(2-3 hours) smart charger is recommended. A 2-3 hour charge time implies a charge rate of 0.5C-0.3C. The smart charger is built to protect the battery from over-charging. They also state that a charge rate of 0.1C for 12-14 hours is well suited. In both cases, once the battery has reached full charge, a trickle charge of less than 0.025C is recommended. Trickle charging means that the batteries gets charged on and off between two voltage levels. The very small trickle charge is used to reduce the negative effects of over-charging and to compensate for the self discharge.

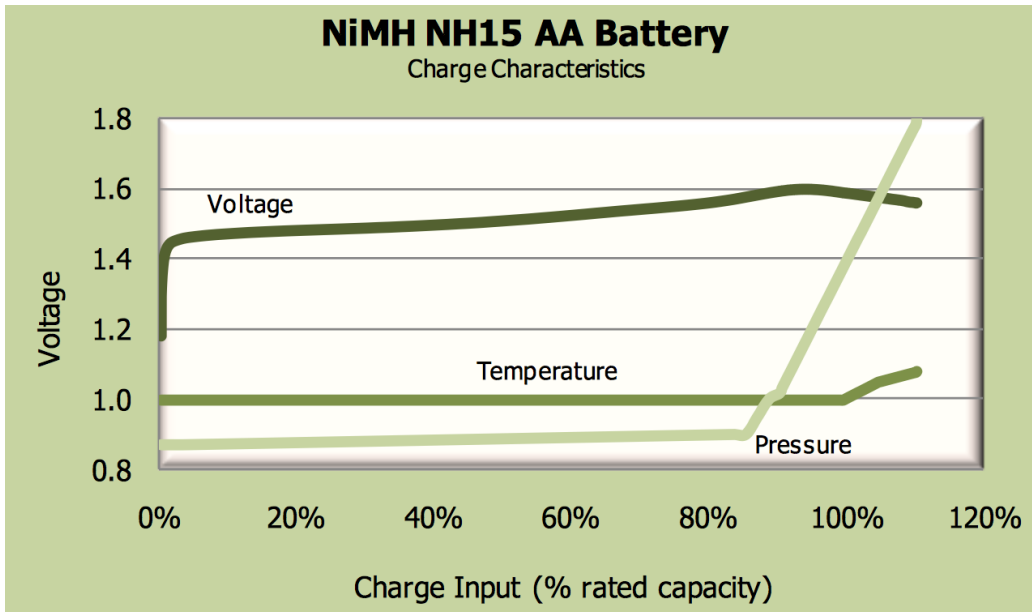


Figure 6: Charging characteristics with a charge rate of 1C. Figure taken from energizer.com.

2.7 Discharge characteristics of NiMH-battery and its effect on capacity measurement

Two important factors when estimating the capacity of a battery are the discharge rate and the ambient temperature. When the estimated capacity of a battery is determined, it should be done with a discharge rate of 0.2C in room temperature.

Figure 2 shows a typical discharge curve of a NiMH-battery being discharged with the conditions explained above. After the initial voltage drop, the voltage of the battery is relatively stable until it reaches the knee of discharge.

Figure 7 shows how the actual capacity of the battery compared to the rated capacity varies with temperature. It can easily be seen that lower temperatures have a larger effect on the capacity than higher temperatures and that there is a significant decrease below 10 degrees.

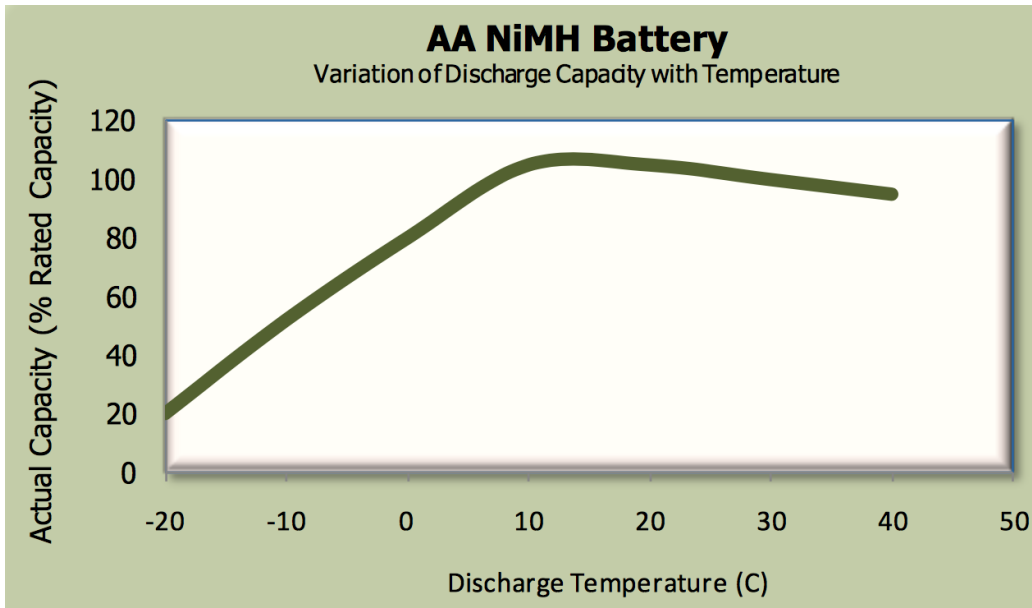


Figure 7: Capacity variation based on temperature. Figure taken from energizer.com.

Figure 8 shows how the actual capacity of the battery compared to the rated capacity varies with the discharge rate used. It can be seen that the actual capacity varies linearly with the discharge rate used.

Another factor that needs to be taken into consideration is the end of discharge voltage. The end of discharge voltage will have an effect on the capacity, where the lower it is, the higher the measured capacity will be. For long term discharge profiles, where the discharge rate is less than 1C, it is recommended to set the cutoff voltage to 0.9 volts per battery cell to avoid the risk of permanent damage to the battery. Figure 9 shows the voltage profile of a battery cell that has been discharged too deep. To avoid damage it is important to stop before the second plateau.

2.8 Self Discharge Characteristics

In an Assa Abloy slider door, the battery pack is trickle charged which ensures fully charged condition. If trickle charge is turned off for a period of time, e.g. 60 minutes, the voltage of the battery will decrease and later on

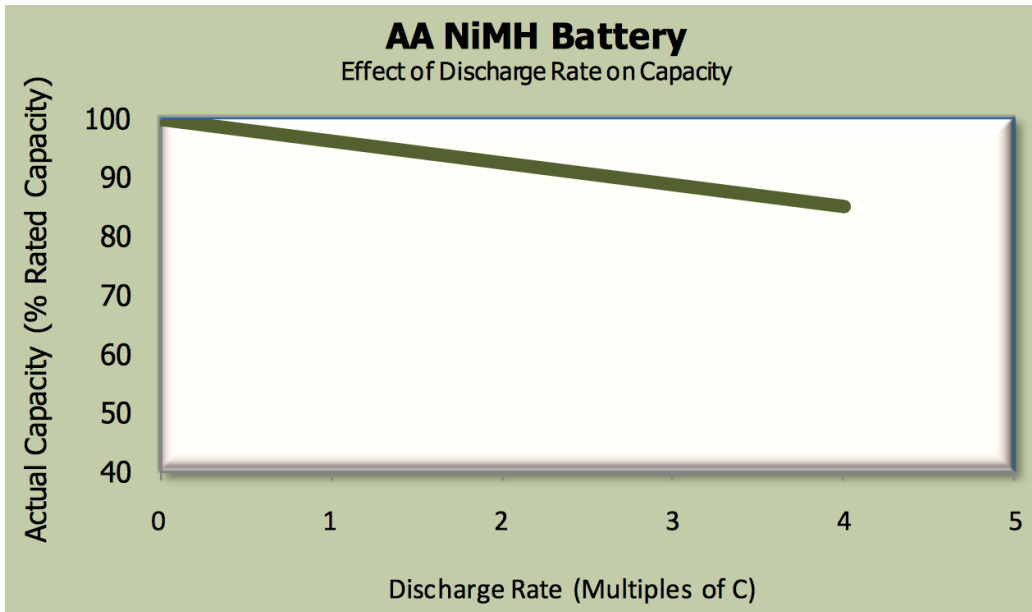


Figure 8: Capacity variation based on discharge rate. Figure taken from energizer.com.

stabilize. There is a scientific report which states that the rate of self discharge correlates to a battery's state of health, i.e. its ability to store energy expressed in Ah [5]. According to the hypothesis, the probability of a battery failure is correlated to the capacity and therefore the self discharge rate is of interest. In order to quantify the self discharge rate, the self discharge rate is measured as the voltage drop occurring during 30 minutes from the moment that the trickle charge is turned off. The battery is in fully charged condition when the trickle charge is turned off. The time of 30 minutes was chosen by studying the self discharge..e curvature for all batteries, see Appendix A.5. It can be seen that the self discharge does not stabilize within this period of time which ensures comparability in self discharge rate.

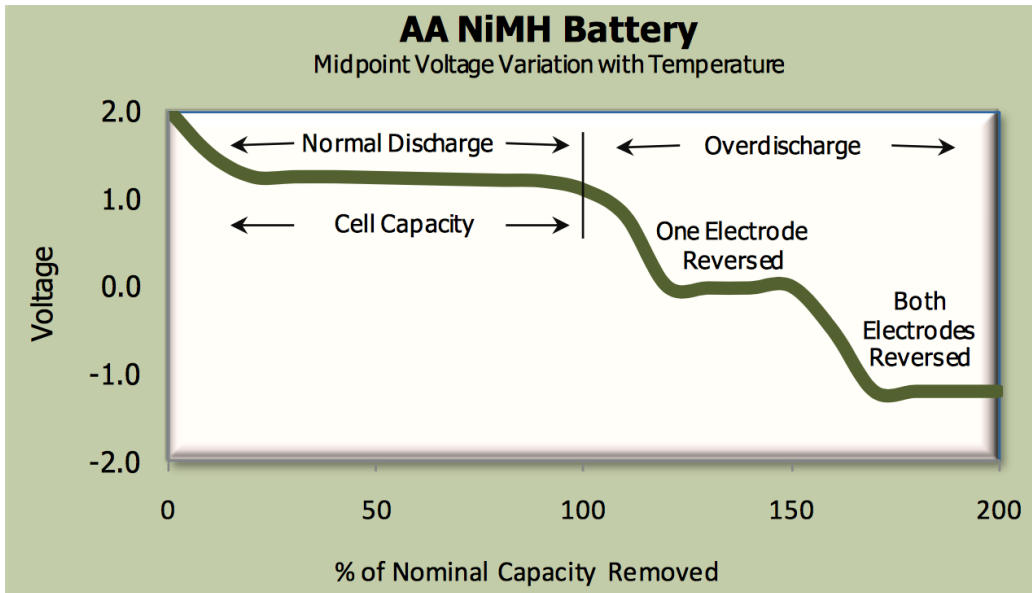


Figure 9: Discharge profile of a battery cell that has been discharge too deep. Figure taken from energizer.com.

3 Methodology

3.1 Investigation

At the start of the project most of the time was committed to investigation. Which parameters were the important ones that could give an indication of the health of the battery? Which methods were needed to calculate these parameters? The company supervisor had some documentation regarding parameters and methods to look at and it was thus investigated if there were any other parameters and methods that could be of value.

3.2 Acquisition of battery data

Once the initial investigation phase was completed, the expected sequence of procedure ended up as described below. Flow chart for acquisition of battery data can be seen in figure 10.

1. Charge batteries with a battery charger rack commonly used at Assa Abloy.
2. Top-charge the batteries with a low current to 14.6V or until they show no sign of progression while continuously measuring the voltage.
3. Turn off the charge and let them self discharge for a set amount of time or until they reach 14.0V while continuously measuring the voltage.
4. Measure internal resistance with Dual Pulse Method.
5. Measure internal resistance with High Current Method.
6. Measure capacity indicator with method described in section 2.4.2
7. Measure capacity of battery using recommended guidelines described in 2.4.1.
8. Analyze data!

Acquisition of battery data

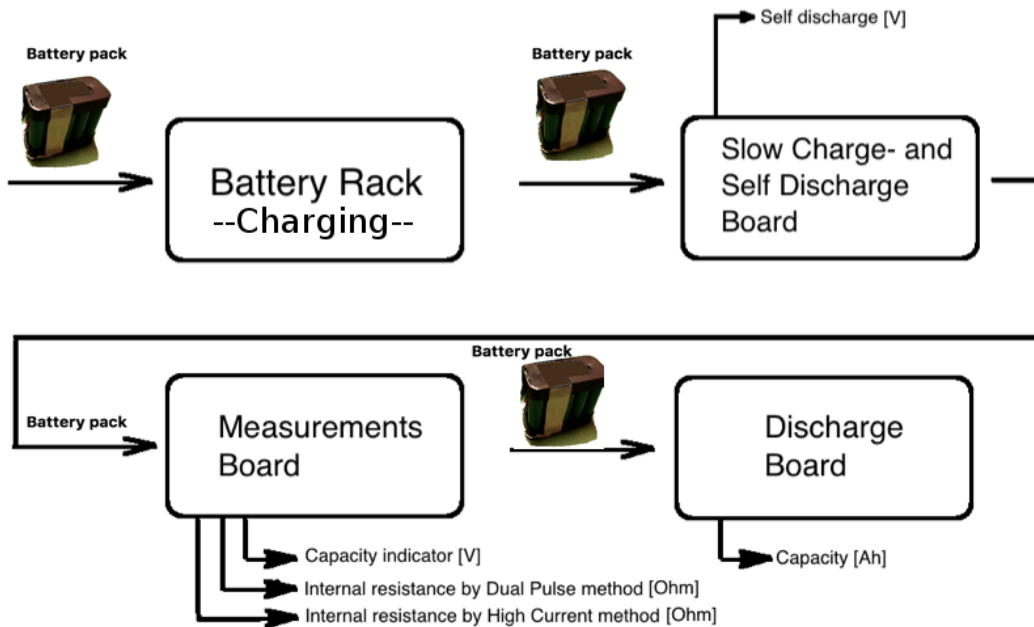


Figure 10: Flow chart for a battery where acquisition of battery data is performed.

In order to do these measurements, the following hardware and functions were needed:

- A microcontroller.
- High precision voltage measurement
- A function to store data during all phases.
- Circuit board to slowly charge batteries to 14.6V.
- Circuit board to measure self discharge phase.
- Circuit board to measure internal resistance and capacity indicator.
- Circuit board to measure capacity of battery.

3.3 Battery performance

The overall goal of this master thesis is to predict battery failure in an Assa Abloy slider door, therefore the batteries are tested in a slider door to examine battery performance. In order to introduce comparability and performance quantification of a battery pack, the measurable figure was chosen to be the number of consecutive openings a battery can do until battery failure occurs. The procedure to retrieve number of door openings per battery pair is close to similar as procedure to "Acquisition of battery data". Instead of capacity measurement the battery pack is mounted in a slider door and performs consecutive door openings until battery failure occurs. The flow chart is seen in figure 11.

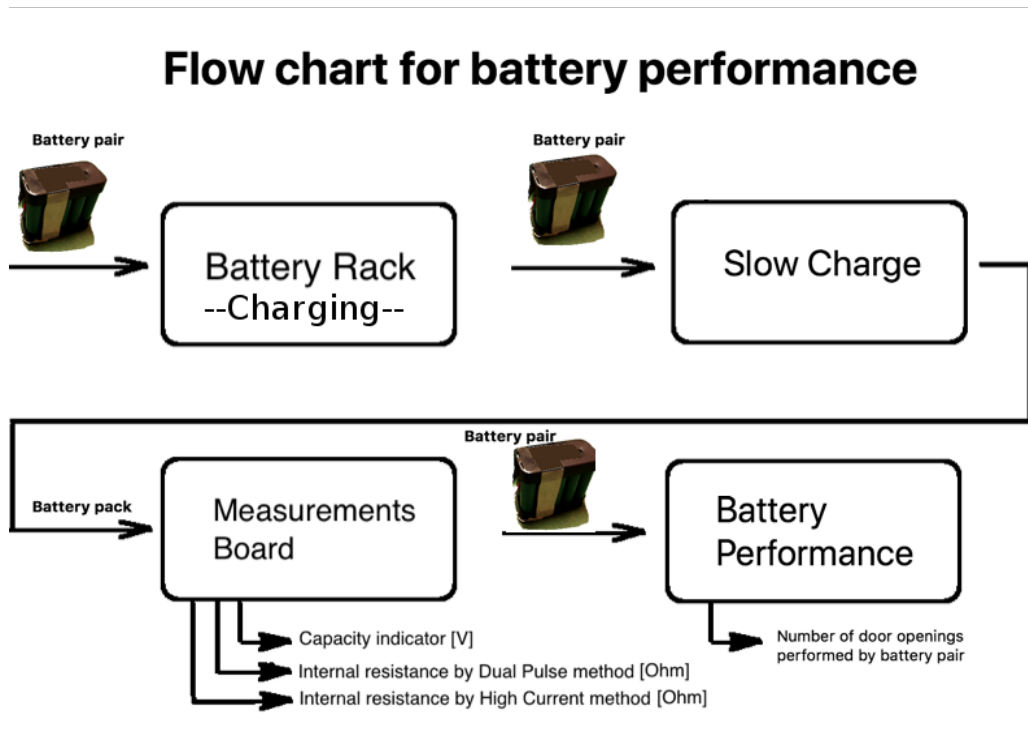


Figure 11: Flow chart for evaluation of battery performance.

3.4 Design of hardware

In the following sub-chapter, the design of the boards are presented.

3.4.1 Choice of microcontroller

At an early stage it was decided to use an Arduino Mega which has an ATmega 2560 on its board. The reason why an arduino was chosen was mostly because of its easy start-up and our experience working with it. The easy possibility of using an SD-card was also another factor, because it was an easy way to store data. It is important to know that the ATmega2560 can only measure up to 5V on its ADC pins. Since the batteries' voltage reaches approximately 14.6V, the voltage has been divided with two resistors to not damage the microcontroller.

3.4.2 Slow Charge and Self Discharge PCB

$$U_{BAT} = U_{arduino} * (1 + R_5/R_4) \quad (11)$$

The current the battery is charged with will vary with the voltage of the battery. However, since the batteries have been fast charged before they are attached to this board, most of them will be close to 13.6V. The software also checks to make sure the battery's voltage is higher than 13.0V. If it is not, the charge is not turned on since the battery is considered to be bad. Using figure 12 as reference, the charge current is calculated as:

$$I_{charge} = (V_1 - U_{BAT} - U_{Q2}) / (R_1 + R_2 + R_3) \quad (12)$$

The board itself has ten identical circuits as shown in figure 12.

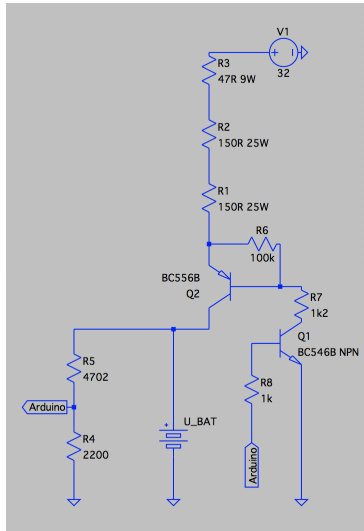


Figure 12: Slow Charge and Self Discharge Board

3.4.3 Measurements PCB

The measurements board has been designed to be able to get the data needed for the "Dual-Pulse Method", "High-Current Method" and "Capacity Indicator Method". Figure 13 shows the design of the board.

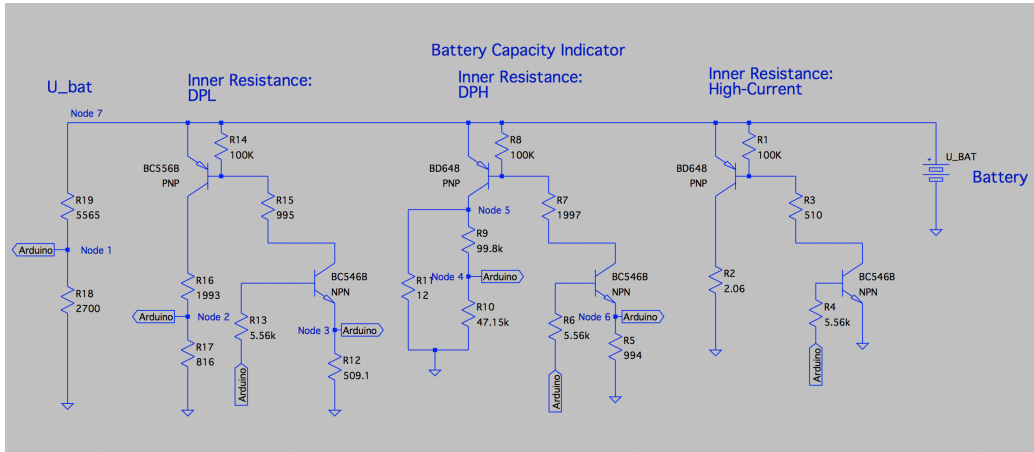


Figure 13: Measurements Board

The Dual-Pulse Method is described in detail in chapter 2.5.1. Equation 8 is used to measure the internal resistance. To acquire U_H and I_H , the circuit named DPH in figure 13 is used. A signal is sent from the microcontroller to the NPN transistor which also makes the PNP transistor above conduct. The current I_H drawn from the battery is the sum of the current running through R_5 and R_{11} .

$$I_H = I_{R_5} + I_{R_{11}} \quad (13)$$

When the current I_H is drawn, $U_H = U_{BAT}$ in figure 13. To acquire U_L and I_L , it is done in the same way but using the DPL circuit in figure 13.

$$I_L = I_{R_{17}} + I_{R_{12}} \quad (14)$$

$U_L = U_{BAT}$ when I_L is drawn.

The High-Current Method is described in detail in chapter 2.5.2. In this case, it has not been designed to fully follow the theory, but instead to what is available to do in Assa's slider doors. In their slider doors, they can draw a peak of 7A and the circuit has therefore been designed to draw a high current but not exceed 7A. Referring to the High-Current circuit in figure 13, the theoretical maximum current that can be drawn is:

$$I_{max} = (U_{OCV} - U_{BD648})/R_2 \quad (15)$$

The current drawn for the closed circuit voltage is calculated according to:

$$I_{CCV} = (U_{CCV} - U_{BD648})/R_2 \quad (16)$$

$U_{OCV} = U_{BAT}$ when the battery is under no load. $U_{CCV} = U_{BAT}$ when a current is drawn through R_2 in figure 13.

Theory of the capacity indicator is described in detail in chapter 2.4.2. The procedure to measure the capacity indicator is as follows: current is conducted through node 5 in figure 13 during five seconds. The battery voltage is sampled continuously. The capacity indicator value is then calculated as the battery voltage when no current is conducted equ. (18), minus the battery voltage when current has been conducted for five seconds. This can be seen in equation (17). It is the impact of equation (19) that results in voltage drop. See figure 21 in results for a graphical illustration of the battery voltage during a capacity indicator measurement sequence.

$$\text{Capacity indicator} = U_{battery}(t = 0) - U_{battery}(t = 5s) \quad (17)$$

$$I_{battery}(t = 0) = 0 \text{ [A]} \quad (18)$$

$$I_{battery}(0 < t \leq 5) = \frac{U_{battery}(t)}{R_{11}} \text{ [A]} \quad (19)$$

R_{11} can be seen in figure 13.

3.4.4 Capacity Measurement Board

The capacity measurement board has been designed to discharge the batteries with a current of approximately 0.2C, according to the theory described in chapter 2.7. Figure 14 shows how each circuit is built. The current drawn from the battery is measured according to the following method:

$$I_{BAT} = U_{BAT}/R_1 = U_{BAT}/47.0 \quad (20)$$

During a capacity measurement, the current drawn will vary as the voltage decreases. The current voltage will decrease from approximately 13V to 9.0V and thus the current will vary accordingly:

$$I_{BAT,start} = 13/47 = 277mA \quad (21)$$

$$I_{BAT,end} = 9/47 = 191mA \quad (22)$$

Since the battery is rated to $C = 1200 \text{ mAh}$, the recommended current, $0.2C$, is equal to:

$$I_{0.2C} = 1200 * 0.2 = 240mA \quad (23)$$

The deviation from the recommended current should not have a big impact on the capacity measurement based on figure 8 in chapter 2.7.

The capacity in Ah is measured based on the current over time according to:

$$C = \int_{T1}^{T2} I_{BAT}/3.6 * dt, \quad (24)$$

where $T2-T1$ is the total time in seconds it took to discharge the battery to $9.0V$. Division by 3.6 is executed to receive the result in mAh.

The board has ten identical circuits to the one shown in figure 14.

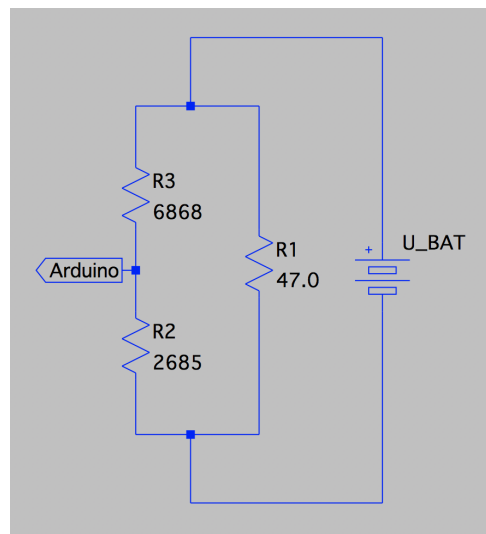


Figure 14: Capacity Measurement Board

3.4.5 Miscellaneous functions

To obtain high precision voltage measurement, an external reference is used. To store data, an arduino shield that supports an SD-card was used. All measured data is stored on the SD-card and then transferred to a computer.

3.5 Verification of circuit boards

Once all of the boards had been designed and built, it was important to verify that each board worked as intended and that correct values were acquired at all positions.

3.5.1 Accuracy of internal resistance measurement

Dual Pulse- and High current method are the two methods employed to measure internal resistance. The internal resistance of a newly produced NiMH battery in an Assa Abloy's slider door is below $1.07R \Omega$. It is then important that the Dual Pulse- and High Current method are able to measure low resistance with good accuracy. To evaluate this a circuit with known resistance was built, see figure 16. This has set-up 1 and set-up 2 with true reference resistance values of:

$$R_{ref1} = 1.123\Omega \quad R_{ref2} = 0.334\Omega$$

See table 3 and 4 in Appendix A.1 for how R_{ref1} and R_{ref2} was calculated.

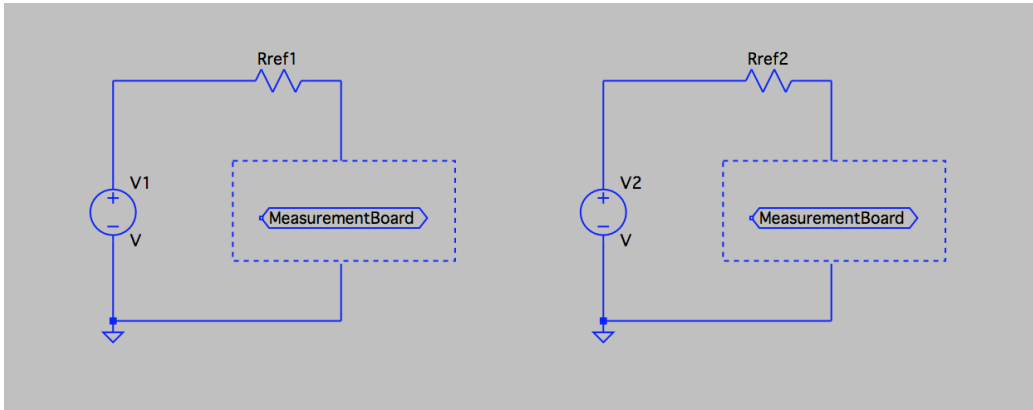


Figure 15: Board with known resistance that is used to test measurement board's accuracy.

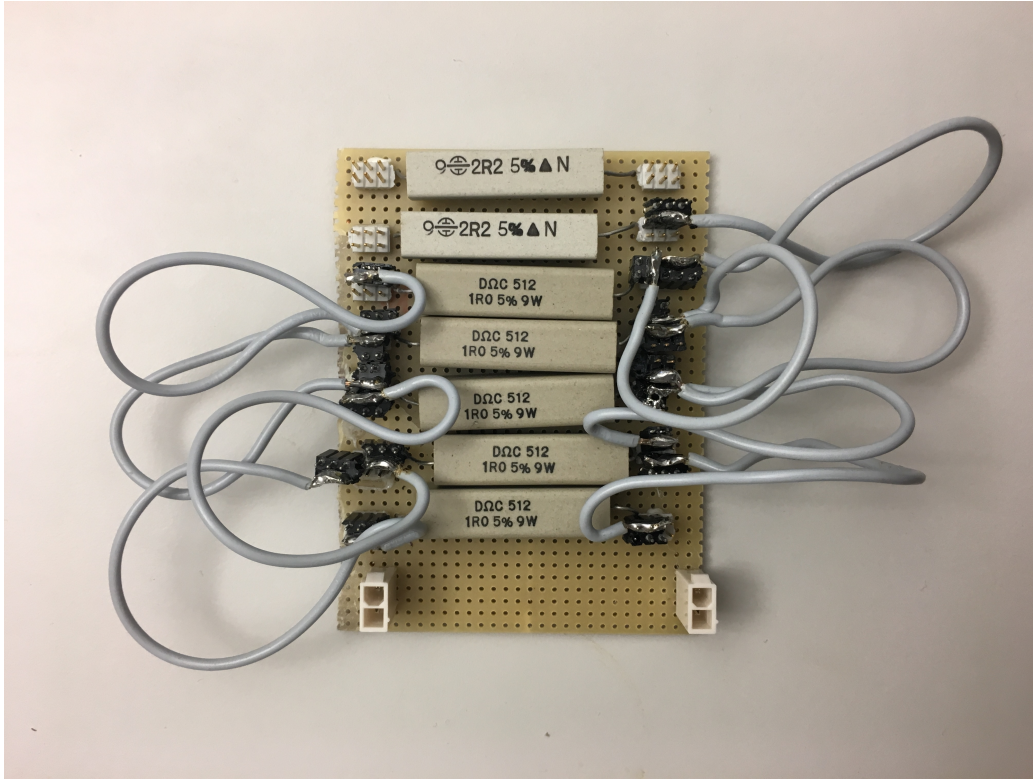


Figure 16: Resistance board that has two set-ups: R_{ref1} and R_{ref2}

3.5.2 Accuracy of battery voltage measurement

This was done with the help of a voltage source with a resolution of one millivolt and a voltmeter with the resolution of ten millivolts. The microcontroller itself has 2^{10} or 1024 discrete steps to measure the voltage, where 1023 will equal 5V. Thus, the resolution of the microcontroller is:

$$U_{\text{DiscreteStep}} = 5.0/1024 = 4.88mV \quad (25)$$

To verify a board, a voltage source was connected to it. Using the measurements board, see figure 13, the voltage source was connected to the board at the far right instead of a battery. The voltage in node 7 was calculated in the following way:

$$U_{VS} = U_{\text{node1}} * (1 + R19/R18) \quad (26)$$

, where U_{VS} is the voltage that the voltage source outputs.

In table 1, U_{Calc} is the calculated voltage at node 7. As can be seen in the table, the average error is 11 mV or 0.107%. The reason why the error is larger than the resolution of the arduino of 4.88 mV is because the error measured in node 1 also gets multiplied by the factor $(1 + R19/R18)$.

Table 1: Verification of voltage measurement

U_VS [V]	U_Calc [V]	U_VS - U_Calc [V]	Error [%]
14	14.005	-0.005	-0.036
13.5	13.512	-0.012	-0.089
13.036	12.989	0.047	0.361
12.975	12.989	-0.014	-0.108
12.342	12.346	-0.004	-0.032
11.943	11.943	0.0	0.0
11.426	11.434	-0.008	-0.070
10.768	10.769	-0.001	-0.009
10.205	10.209	-0.004	-0.039
9.761	9.760	0.001	0.010
8.828	8.819	0.009	0.102
7.490	7.473	0.017	0.227
6.702	6.681	0.021	0.313
	Average	0.011	0.107

The Error has been calculated as:

$$Error = ((U_{VS} - U_{Calc})/U_{VS}) * 100 \quad (27)$$

Similar methods were used to verify all of the boards. In the appendix, more data for all boards can be found.

From Appendix A.1, it can be concluded that the accuracy of Dual Pulse and High-Current method is good. When the resistance board in figure 16 is connected as illustrated in figure 15 the measurement board is able to measure the reference resistance R_{ref1} and R_{ref2} with less than 0.008 Ω deviation. The real value of the resistance was determined by connecting the circuit to a constant voltage source where the current was measured and thereby the true resistance of the circuit.

3.6 Measurement Sequence

In the following chapter, each sequence mentioned in chapter 3.2 is described in more detail. The measurement sequence has been carried out on approximately 200 batteries. Most of these batteries have been returned from service visits due to some, unfortunately, unknown reason. A few of the batteries have been brand new.

3.6.1 Fast charge using Assa Abloy's battery rack

The first phase is the least important one because it is only to quickly charge the batteries to an almost fully charged state. This is done by a battery rack commonly used at Assa Abloy. The battery rack starts by discharging the batteries with a current of 0.63C until it reaches a certain voltage. After that, it charges the battery with a constant current of 0.3C for four hours. During this phase, no data is acquired.

3.6.2 Slow Charge and Self Discharge Phase

The second phase is the Slow Charge and Self Discharge Phase (SCSDP). On this board, the batteries will be top-charged with a current of approximately 0.045C to ideally 14.6V. If the capacity of the battery has been reduced, it will be top charged to whichever voltage it maxes out at. The rate at which the batteries are charged have been designed to match the charge-current used in Assa Abloy's doors. Once a battery reaches its maximum voltage, the Self Discharge Phase (SDP) is initiated. The slow charge is turned off and the battery will self discharge for 60 minutes or until it reaches 14.0V. During both phases, the voltage is continuously measured and saved to an SD-card.

3.6.3 Measurements Phase

Once the SDP has been completed, the next phase is the measurements phase. This involves retrieving data to calculate the internal resistance of the battery using both the Dual Pulse Method and the High Current Method as well as calculating the battery capacity indicator. In figure 13, the measurements board can be seen. Based on which NPN-transistor of the three available conducts, the different circuits will be active.

3.6.4 Capacity Measurement

After the Measurements Phase has been completed, the capacity of the battery is measured. The battery is connected to the Discharge Board where the voltage is continuously measured until it reaches 9.0V.

3.7 Battery performance based on measured parameters

Once all the batteries had gone through the measurements, a large set of data from batteries had been acquired. The two parameters that were anticipated to be the most crucial to the batteries' performance was the internal resistance and the capacity. The question was how well a battery would perform based on the value of these two parameters. Therefore, a set of batteries with varying capacity and internal resistance were chosen to be tested on a "worst case scenario" door; a door with a high peak current and a long distance to travel. The high peak current will result in a high voltage drop during an opening and the long distance will impact the capacity. Figure 17 shows the battery current during one opening.

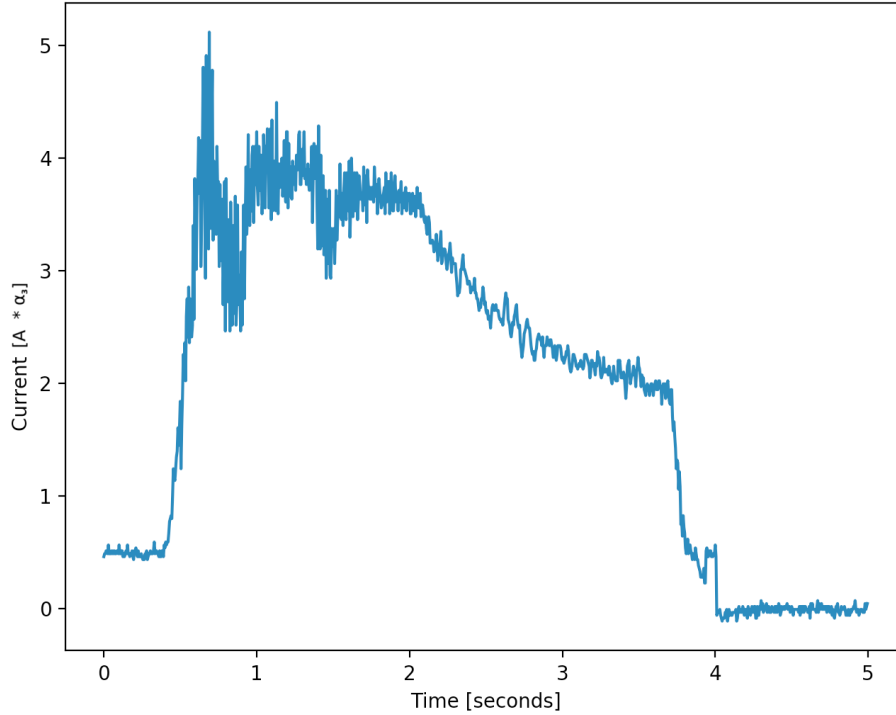


Figure 17: Current output from battery during one opening.

The doors use two battery packs in series and therefore batteries with similar internal resistance and capacity were paired. The idea was to see how many consecutive door openings one pair of battery packs could do based on their internal resistance and capacity. The batteries will fail if the voltage at some point during an opening drops below $11.11\alpha_2$ V.

After an initial test phase it was seen that the number of door openings was strongly correlated to the internal resistance and less so to the capacity. A new test phase was then started where the battery pairs were chosen only based on the internal resistance. This set of batteries was tested in different temperatures and the internal resistance of the batteries was also measured at these temperatures.

4 Results

4.1 Capacity

Figure 18 shows the discharge curves for a number of batteries. The batteries with a high capacity has two very clear knees and a plateau. It can also be seen that the batteries with lower capacity has a greater slope in its plateau than the good ones, which has somewhat of an impact on its performance in the doors. The reason why is explained more in detail in chapter 5.1.

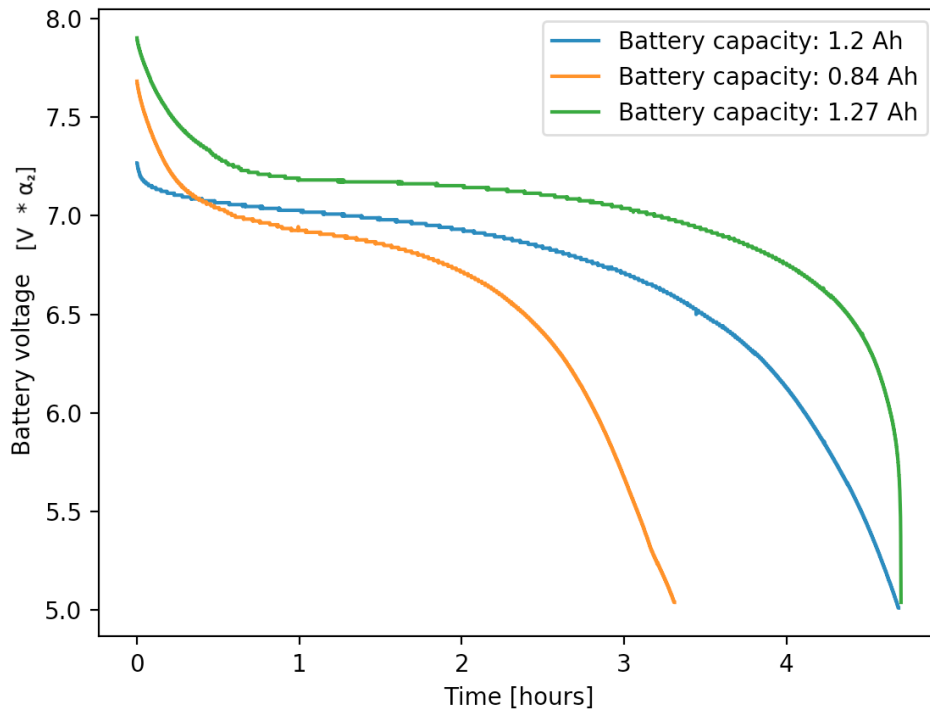


Figure 18: Illustration of discharge characteristics of fully charged NiMH batteries with different Ah.

4.1.1 Self discharge's correlation to capacity

The method used to measure the capacity is not possible to use on a battery in a door. The self discharge measurements were done to see if there was a correlation between the self discharge and the capacity. Figure 19 shows

the self discharge curve for five different batteries and figure 20 shows the correlation between self discharge and capacity.

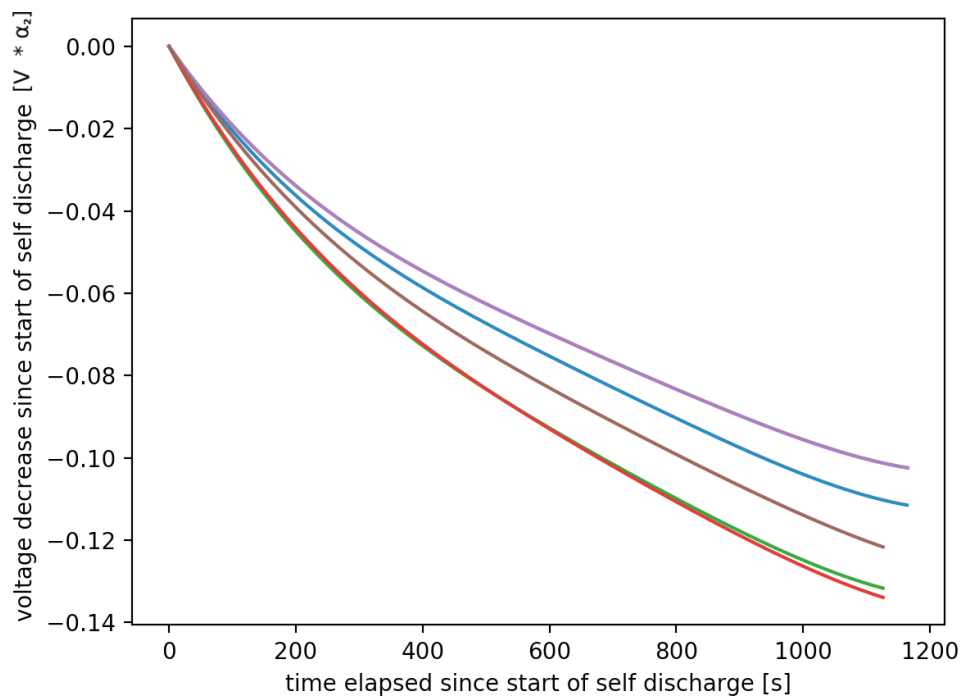


Figure 19: Self discharge curves during first 1100s of time. Full self discharge can be found in Appendix A.5.

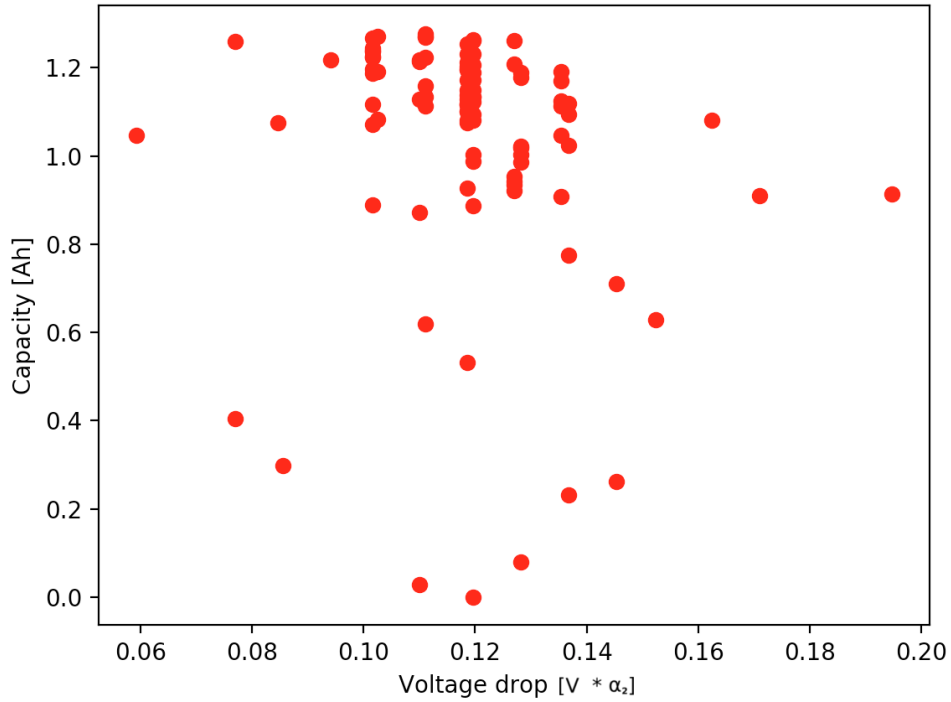


Figure 20: Total voltage drop during self discharge vs capacity

Looking at figure 20, no correlation between the two parameters can be seen.

4.1.2 Capacity indicator's correlation to capacity

The voltage drop of the battery during the capacity indicator measurement sequence is presented in figure 21. Regarding the stated hypothesis, it is interesting to examine the correlation between battery performance and capacity indicator, see figure 22.

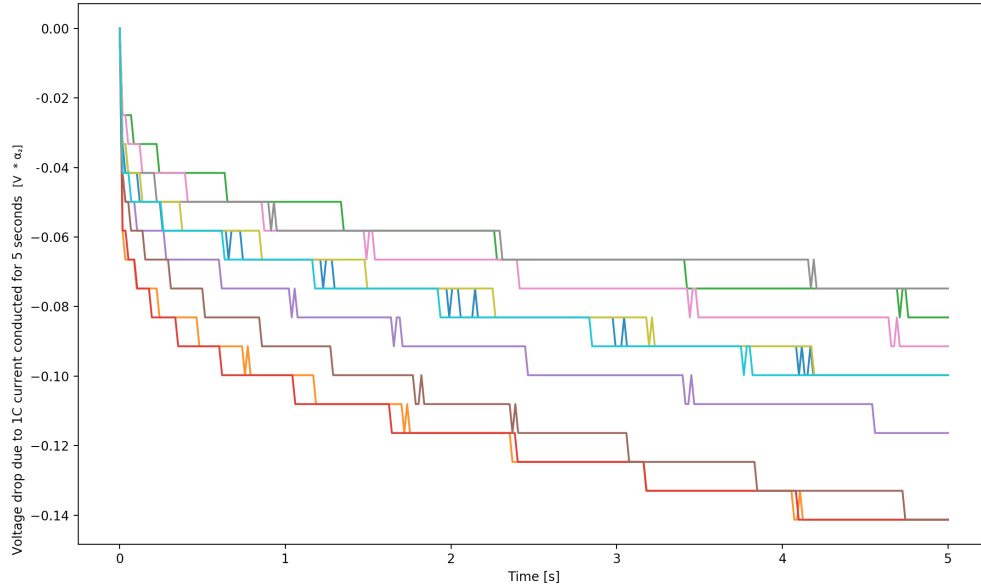


Figure 21: Voltage drop during capacity indicator measurement sequence. Each line represents one battery pack.

4.1.3 Capacity indicator's correlation to door openings

Correlation between a battery's capacity indicator value and it's ability to open a door, see figure 22. According to this, a battery with a capacity indicator value lower than $1.0\alpha_2$ V results in a successful door opening.

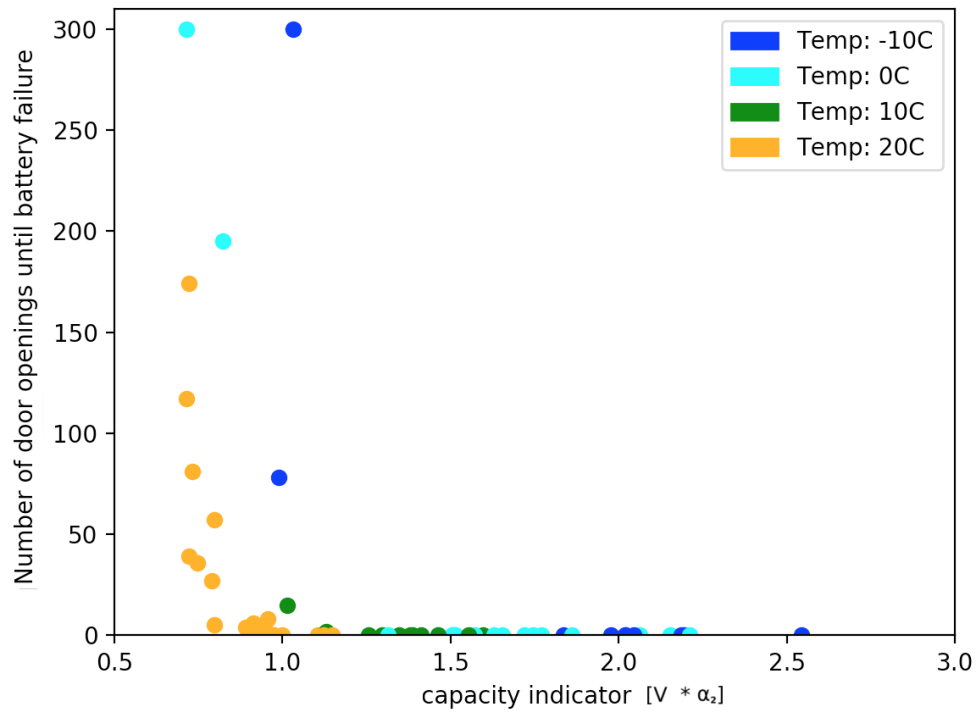


Figure 22: Number of door openings versus capacity indicator value. Each dot represents one battery pair. Note that dots which are located as half circles on the x-axis did perform 0 door openings in this test.

4.2 Age of battery counted from production date

Correlation between age of battery and its performance has been analyzed. The result is seen in figure 23. It is seen that there is no correlation between age and battery failure. This is most likely due to too many other factors affecting the battery; the climate, type of door and rate of usage to name a few.

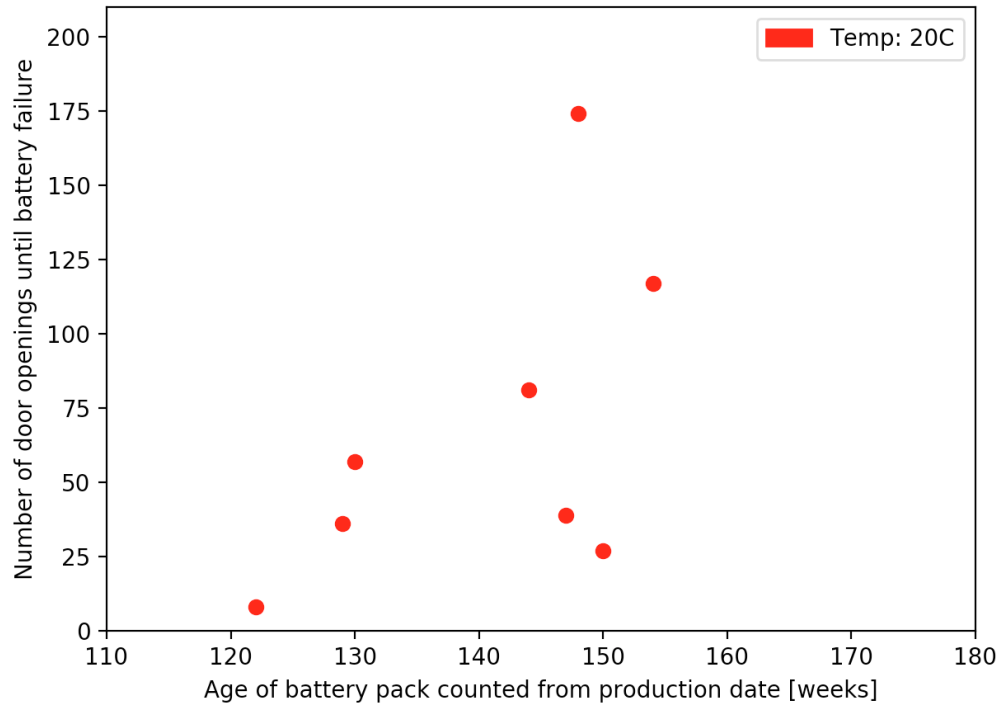


Figure 23: Each dot represents a battery pair that has been through door opening phase where its production date is known.

4.3 Internal Resistance

The internal resistance of the batteries have been measured with two different methods; the Dual Pulse Method and the High Current Method. Figure 24 shows the correlation of the internal resistance between the methods. It can be seen that there is a strong correlation between the two and almost a linear relationship when the internal resistance is less than $1.67\alpha_1 \Omega$ measured by the High Current Method. It should also be noted that there is a static error between the two.

Figure 1

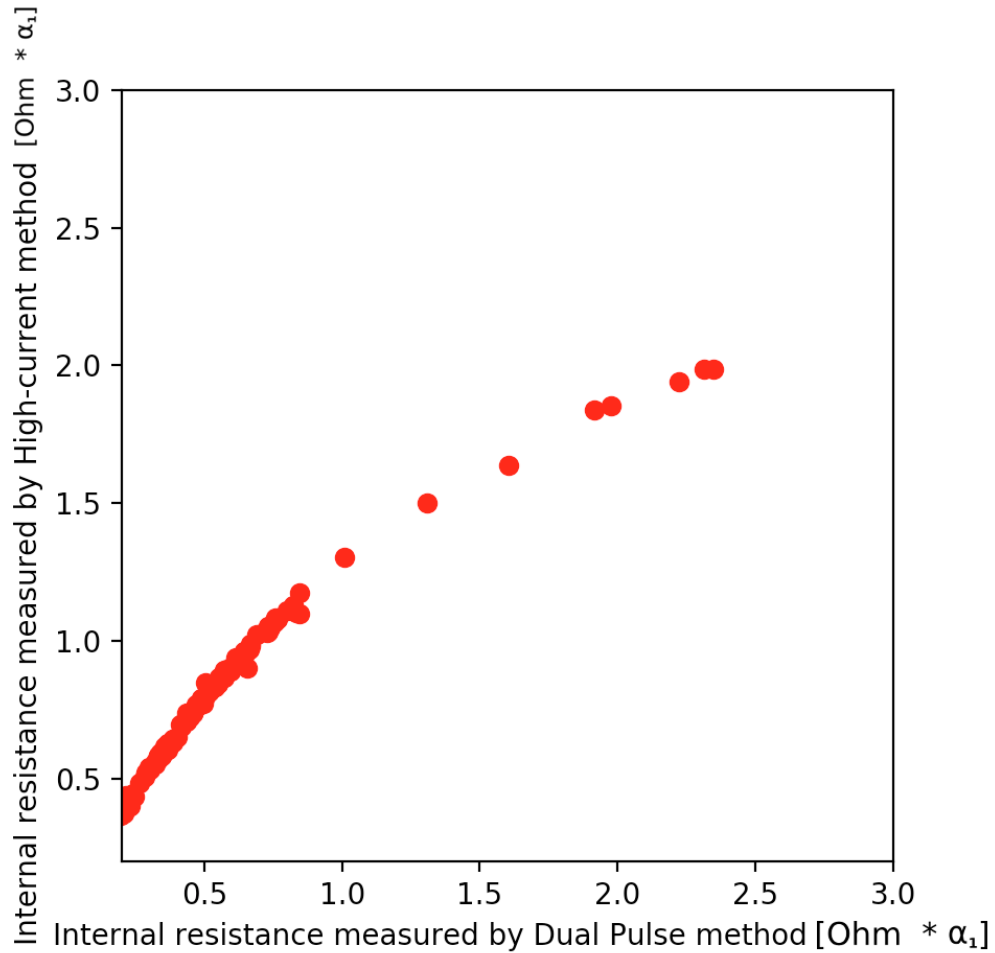


Figure 24: Internal resistance measured by dual pulse- and high current method. Each dot represents a battery pack.

The result of the ten battery pairs that were chosen to go through tests on a door in different temperatures can be seen in figure 25. The internal resistance displayed in the figure is from the Dual Pulse Method.

IR DP-Method -10° C	DO -10° C	IR DP-Method 0° C	DO 0° C	IR DP-Method 10° C	DO 10° C	IR DP-Method 20° C #2	DO 20° C #2	IR DP-Method 65° C	DO 65° C
2,846 α_1	0	2,285 α_1	0	1,701 α_1	0	1,386 α_1	0	0,675 α_1	2
2,285 α_1	0	1,779 α_1	0	1,417 α_1	0	1,139 α_1	0	0,567 α_1	-
2,280 α_1	0	1,827 α_1	0	1,411 α_1	0	1,106 α_1	0	0,567 α_1	3
1,981 α_1	0	1,923 α_1	0	1,513 α_1	0	1,153 α_1	0	0,575 α_1	18
2,003 α_1	0	1,679 α_1	0	1,378 α_1	0	0,942 α_1	6	0,534 α_1	16
1,943 α_1	0	1,487 α_1	0	1,309 α_1	0	1,037 α_1	0	-	-
1,961 α_1	0	1,422 α_1	0	1,212 α_1	0	1,010 α_1	0	-	-
1,803 α_1	0	1,494 α_1	0	1,467 α_1	0	1,011 α_1	3	0,526 α_1	30
0,715 α_1	78	0,647 α_1	195	-	200+	0,573 α_1	200+	-	-
0,621 α_1	165+	0,521 α_1	200+	-	200+	0,449 α_1	200+	-	-

Figure 25: Internal resistance vs door openings

It can be seen that the internal resistance increases as the temperature decreases and that the threshold of the internal resistance when it still manages to do a door opening is somewhere around $1.0\alpha_1 \Omega$. If the internal resistance vs door openings is analyzed in general, it can also be seen that there seems to be a deviation for the $65^\circ C$ test. For instance, at $20^\circ C$ there is a battery pair with $0.573\alpha_1 \Omega$ that does 200+ openings and at $65^\circ C$ there is a pair with $0.575\alpha_1 \Omega$ that does 18. The reason why it does not seem to behave in a similar way at $65^\circ C$ is discussed in chapter 5.3.

A second set of batteries were chosen to go through tests on a door to strengthen the result from the previous set. Due to lack of time, they were only tested at $0^\circ C$ and $10^\circ C$. The result is shown in table 2.

Table 2: Internal resistance vs door openings

IR DP-Method $0^\circ C$ [Ω]	DO $0^\circ C$	IR DP-Method $10^\circ C$ [Ω]	DO $10^\circ C$
1.446 α_1	0	1.081 α_1	0
1.183 α_1	0	0.917 α_1	15
2.454 α_1	0	1.635 α_1	0
1.484 α_1	0	1.238 α_1	0
1.657 α_1	0	-	-
1.613 α_1	0	-	-
1.639 α_1	0	-	-
-	-	0.979 α_1	16

Figure 26 shows the correlation between the internal resistance and number of door openings for all tests that were done except for the $65^\circ C$ one. It can be seen that there seems to be a threshold for the internal resistance at

approximately $1.0\alpha_1 \Omega$ or $1.7\alpha_1 \Omega$, depending on if the Dual-Pulse Method or the High Current Method is used, for when the door no longer manages to open the door.

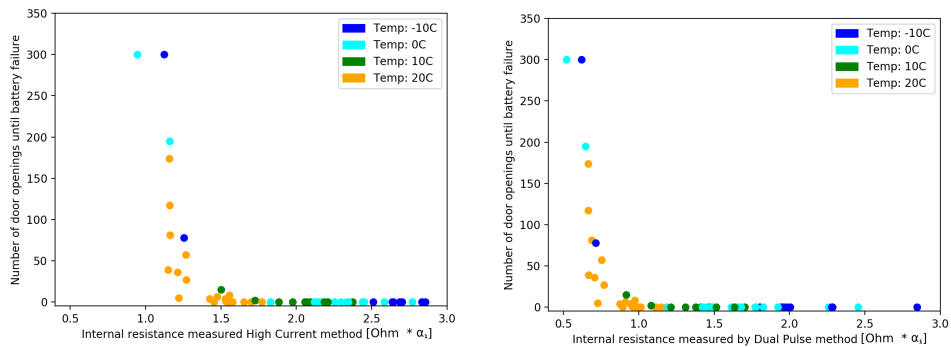


Figure 26: Internal resistance vs door openings

4.4 Temperature

A battery generates power by a chemical reaction. Since temperature has impact on chemical reactions and electrical characteristics such as resistance, it is of interest to examine temperature impact on a battery's characteristics. See figure 27, 28 and 29 on how temperature impacts on respectively: capacity indicator, internal resistance measured by dual pulse- and high current method.

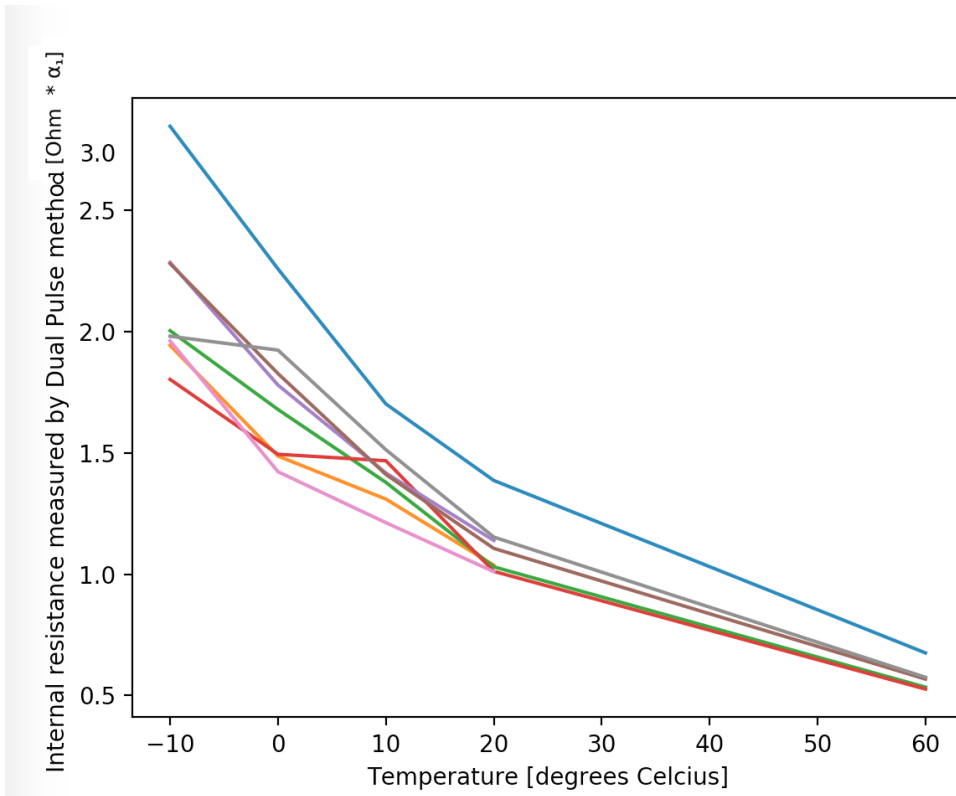


Figure 27: Temperature impact on internal resistance measured by Dual Pulse method. Each line represents a unique battery pair.

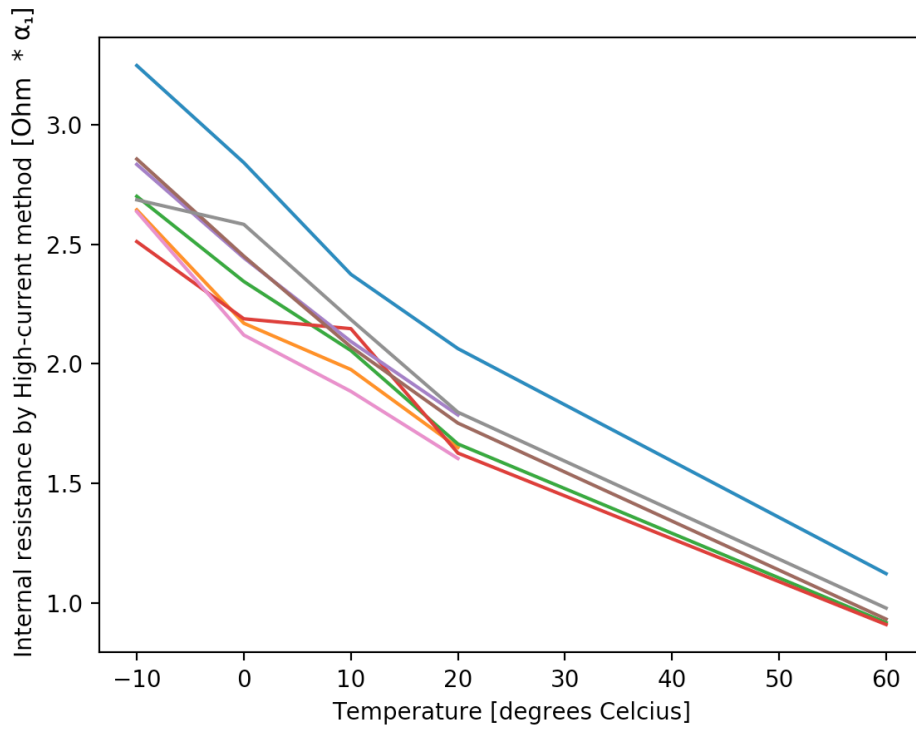


Figure 28: Temperature impact on internal resistance measured by High Current method. Each line represents a unique battery pair.

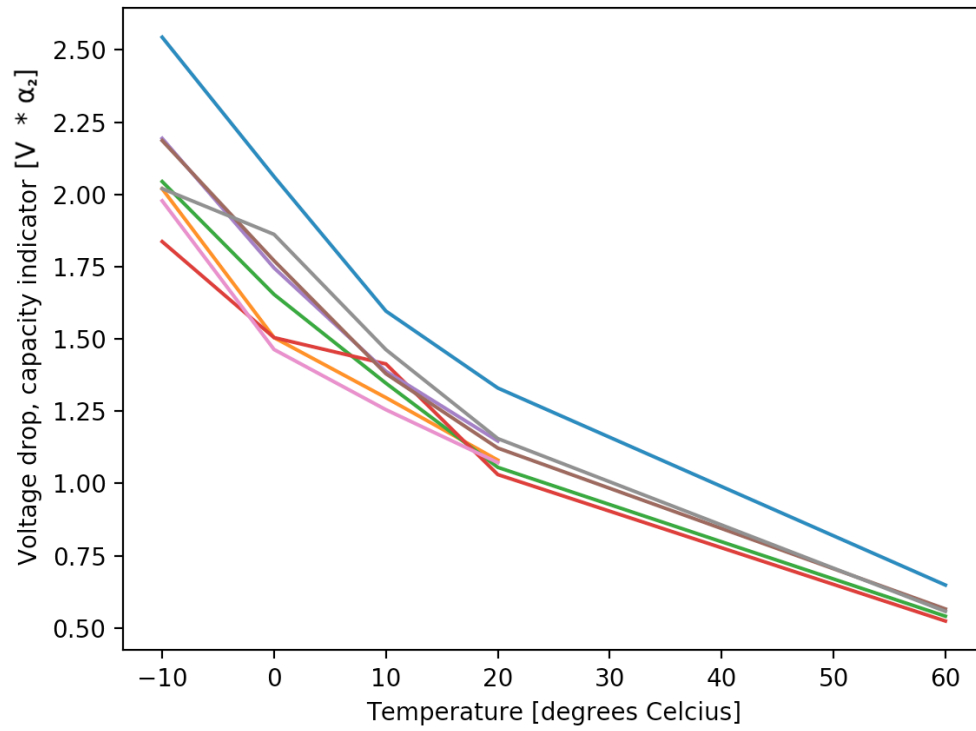


Figure 29: Temperature impact on capacity indicator. Each line represents a unique battery pair.

5 Discussion

5.1 The capacity's impact on battery performance

The capacity has according to the investigation in this master thesis no impact on the battery's performance to open a door once or not. The capacity is the energy stored in the battery and does not correlate to the power it can deliver. Another idea was that the internal resistance and the capacity correlates. By studying figure 30 it can be seen that there is no apparent correlation between the two parameters.

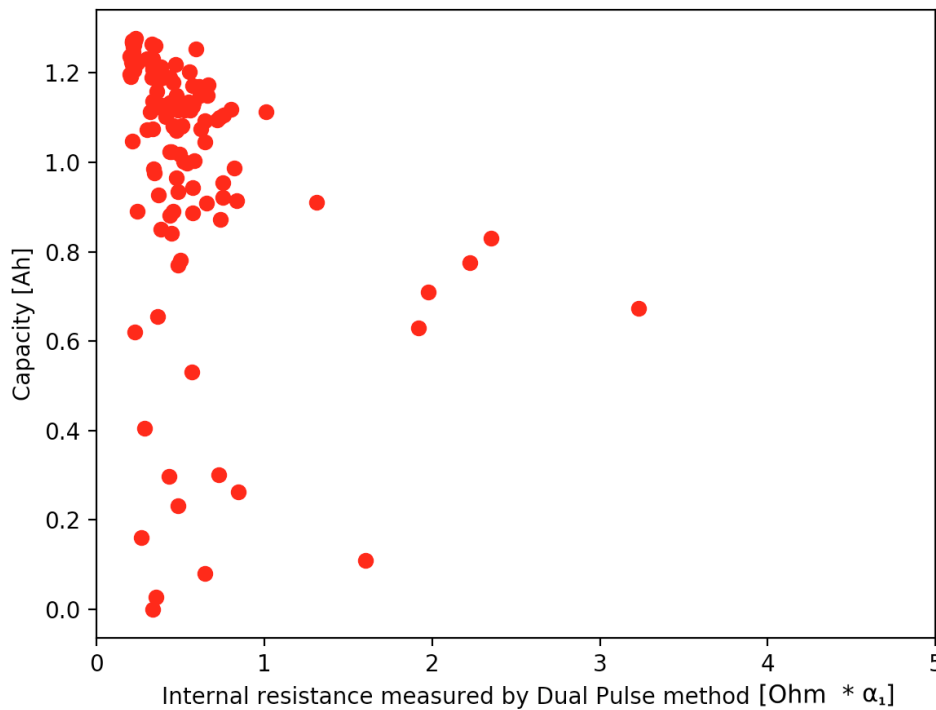


Figure 30: Internal resistance using DP-Method vs capacity

5.2 Capacity indicator's correlation to battery performance

The capacity indicator is the method employed in order to examine hypothesis number 2, which says:

”The likelihood of battery failure is correlated to the magnitude of a voltage drop occurring from current conducted from a battery during a five seconds period.”

In figure 22, it can be seen that the capacity indicator does correlate to the probability of battery’s failure. This validates the stated hypothesis. According to figure 22, a capacity indicator value less than $1.11\alpha_2$ V does ensure that the door will be able to open.

5.3 The temperature’s impact on the open circuit voltage

As mentioned in chapter 4.3, it could be seen that the tests carried out at $65^{\circ}C$ did not behave in the same way as the other temperatures. It was seen that two battery pairs with very similar internal resistance, but measured at $20^{\circ}C$ and $65^{\circ}C$, had a big discrepancy in the amount of door openings. What was observed and what is believed to be the reason, is that when a battery pack is charged at $20^{\circ}C$ versus $65^{\circ}C$, the open circuit voltage is significantly lower for the $65^{\circ}C$ case when using Assa’s charge algorithm. Because it was observed at a late stage during the master thesis, no documentation of this has been done and it should be said that this is only a hypothesis. Further investigation needs to be done to verify this.

5.4 Conclusions

The results has been presented and discussion upon them have been employed. With knowledge from this it is now appropriate to draw conclusions in a failure prediction perspective.

5.4.1 Internal Resistance’s impact

The parameter that showed the strongest correlation to the performance of the batteries was the internal resistance. The reason why is because when the internal resistance increases, much power is lost and the powered delivered decreases. When opening a door, high power during a short period of time is needed. This means that the internal resistance affects the likelihood of a battery failure, which answers hypothesis 1.

5.4.2 Capacity's impact

The conclusion is that the capacity does not have any correlation to the performance of the batteries. If the battery can't deliver a power high enough, it doesn't matter if the battery has a high capacity. This means that the capacity does not affect the likelihood of a battery failure, which answers hypothesis 3.

5.4.3 Temperature's impact

The temperature does have a strong correlation to the performance of the battery because it strongly affects the internal resistance of the battery. Thus, when the battery is under a load, there will be a voltage loss which is dependent on the internal resistance. This means that the temperature affects the likelihood of a battery failure, which answers hypothesis 5.

5.4.4 Age's impact

The age of the battery does not have any correlation to the performance of the battery. This means that the age of the battery does not affect the likelihood of a battery failure, which answers hypothesis 4.

5.4.5 Capacity Indicator's impact

The capacity indicator method shows a correlation to the performance of the battery. When the capacity indicator value decreases, the performance of the battery increases. It thus affects the likelihood of a battery failure, which answers hypothesis 2. The reason why, is because it basically is a measurement of the internal resistance.

5.4.6 Failure prediction - What is needed?

As seen in the previous chapter, it is quite straight forward to calculate if the door will succeed or not. All of the three parameters needed can be measured in real-time. However, to **predict** battery failure, the following needs to be known:

- The correlation between temperature and internal resistance
- The correlation between time/aging and internal resistance

- The correlation between temperature and the peak battery voltage with no load.

To be able to predict battery failure, Assa Abloy is recommended to do the following:

- Collect a set of new battery pairs and measure the internal resistance at different temperatures to see how the internal resistance correlates to the temperature.
- Implement measurement of the internal resistance in their slider doors and after a couple of months crunch the data to see if any correlation between age and internal resistance can be found.
- Collect a set of new battery pairs and measure the battery voltage at different temperatures, using the same charge-algorithm as used in the door. This is done to see how the battery voltage correlates to the temperature.

References

- [1] mpoweruk.com/soh.htm, (2005). *State of Health Determination*. [online] Available at: <http://www.mpoweruk.com/soh.htm> [Accessed 20 Oct. 2017].
- [2] Energizer, (2010). *NiMH - Handbook and Application Manual* [pdf]. Available at: http://data.energizer.com/pdfs/nickelmetalhydride_appman.pdf [Accessed 25 Sep. 2017]
- [3] Tarabay, J., Karami, N. (2015). *Nickel Metal Hydride battery: Structure, chemical reaction, and circuit model*. [online] Available at: <http://ieeexplore.ieee.org.ludwig.lub.lu.se/xpls/icp.jsp?arnumber=7113594> [Accessed 25 Oct. 2017]
- [4] Energizer, (2005). *Battery Internal Resistance* [pdf]. Available at: <http://data.energizer.com/pdfs/batteryir.pdf> [Accessed 20 Sep. 2017]
- [5] Yamashita, A. et al. (2005). *Capacity Estimation and Lifetime Expectancy of Large-Scale Nickel Metal Hydride Backup Batteries*. [online] Available at: <http://ieeexplore.ieee.org.ludwig.lub.lu.se/document/4134346/?reload=true>

A Verification data

A.1 Internal resistance measurement

By applying various voltage levels with a power supply to the resistance circuit board in figure 16 on page 29, true resistance value for set-up 1 and 2 was retrieved, see table 3 and 4.

$$R_{ref1} = 1.123\text{Ohm} \quad R_{ref2} = 0.334\text{Ohm}$$

These two values will serve as reference values to evaluate the accuracy of the internal resistance measurement methods.

Table 3: measurements to evaluate reference resistance value for R_{ref1} .

Power supply [V]	Setup 1- current [A]	Setup 1 -Resistance of resistance board [Ω]	Setup 1 - standard deviation [Ω]	Setup 1 - average resistance [Ω]
0,202	0,18	1,12		
0,315	0,28	1,13		
0,431	0,38	1,13		
0,559	0,5	1,12		
1,272	1,14	1,12		
2,072	1,85	1,12		
			0,00719	1,123

Table 4: Measurements to evaluate reference resistance value for R_{ref1} .

Power supply [V]	Setup 2 - current [A]	Setup 2 - Resistance of resistance board [Ω]	Setup 2 - standard deviation [Ω]	Setup 2 - average resistance [Ω]
0,112	0,34	0,329		
0,36	1,11	0,324		
0,453	1,35	0,336		
0,19	0,56	0,339		
0,292	0,87	0,336		
			0,00593	0,333

Table 5: Measurement of R_{ref1} with Dual Pulse method.

Voltage DPH [V]	Voltage DPL [V]	Upset 1- Resistance measured by Dual Pulse [Ω]	Standard deviation of measured resistance	Average value [Ω]
6,13	6,63	1,13		
9,29	10,08	1,13		
11,97	13	1,12		
12,75	13,85	1,13		
12,81	13,91	1,12		
			0,00547	1,126

Table 6: Measurement of R_{ref2} with Dual Pulse method.

Voltage DPH [V]	Voltage DPL [V]	Upset 2 -Resistance measured by Dual Pulse [Ω]	Standard deviation of measured resistance	Average value [Ω]
6,48	6,63	0,32		
9,61	9,84	0,33		
11,54	11,82	0,32		
12,45	12,76	0,33		
13,58	13,93	0,33		
			0,00547	0,326

Table 7: Measurement of R_{ref2} with High-Current method.

Voltage in node 7 when no current is conducted [V]	Voltage in node 7 when current is conducted through High-Current branch	Upset 2 - Resistance measured by High-Current [Ω]	Standard deviation of measured resistance	Average value [Ω]
9,75	8,684	0,326		
11,7	10,403	0,325		
13,64	12,136	0,328		
			0,00152	0,326

A.2 Verify Measurements Board

DPH/Capacity Indicator Circuit							
U_VM = U_VoltMeter							
U_Voltage Source	U_VM_node7	U_Calc_node7	Node 7 - Error [%]	U_VM_node4	U_Calc_node4		Node 4 - Error [%]
	14	13,86	13,871	0,079	4,16	4,175	0,361
	13,735	13,59	13,602	0,088	4,076	4,092	0,393
	13,562	13,42	13,422	0,015	4,02	4,038	0,448
	13,273	13,14	13,138	0,015	3,933	3,95	0,432
	12,949	12,82	12,824	0,031	3,83	3,848	0,470
	12,393	12,27	12,271	0,008	3,655	3,672	0,465
	11,978	11,85	11,868	0,152	3,525	3,54	0,426
	11,655	11,53	11,539	0,078	3,423	3,438	0,438
	11,137	11,02	11,031	0,100	3,26	3,271	0,337
	10,647	10,54	10,538	0,019	3,106	3,115	0,290
	10,283	10,18	10,179	0,010	2,991	2,998	0,234
	9,747	9,65	9,641	0,093	2,823	2,827	0,142
	9,275	9,18	9,177	0,033	2,674	2,681	0,262
	8,579	8,49	8,475	0,177	2,455	2,456	0,041
	7,862	7,78	7,772	0,103	2,229	2,231	0,090
			Average:	0,067		Average:	0,322
			Median:	0,078		Median:	0,361
U_Voltage Source	U_VM_node6	U_Calc_node6	Node 6 - Error [%]				
	14	4,1	4,106	0,146			
	13,735	4,032	4,033	0,025			
	13,562	3,982	3,984	0,050			
	13,273	3,901	3,901	0,000			
	12,949	3,808	3,813	0,131			
	12,393	3,649	3,652	0,082			
	11,978	3,53	3,53	0,000			
	11,655	3,435	3,438	0,087			
	11,137	3,287	3,286	0,030			
	10,647	3,147	3,145	0,064			
	10,283	3,041	3,042	0,033			
	9,747	2,887	2,886	0,035			
	9,275	2,75	2,749	0,036			
	8,579	2,549	2,544	0,196			
	7,862	2,341	2,334	0,299			
			Average:	0,081			
			Median:	0,050			

Figure 31: Verification of DPH/Capacity Indicator Circuit

DPL Circuit					
U_VoltageSource [V]	U_Calc_node7 [V]	Node 7 Error [%]	U_VM_node2 [V]	U_Calc_node2 [V]	Node 2 Error [%]
14	14,005	0,036	4,059	4,0625	0,086
13,562	13,557	0,037	3,936	3,931	0,127
13,171	13,168	0,023	3,818	3,823	0,131
12,928	12,929	0,008	3,747	3,75	0,080
12,344	12,346	0,016	3,578	3,579	0,028
11,788	11,793	0,042	3,417	3,418	0,029
11,233	11,24	0,062	3,256	3,257	0,031
10,527	10,523	0,038	3,051	3,052	0,033
	Average:	0,033		Average:	0,068
	Median:	0,036		Median:	0,056
U_VoltageSource [V]	U_VM_node 3 [V]	U_Calc_node3 [V]	Node 3 Error [%]		
14	4,2	4,214	0,333		
13,562	4,19	4,189	0,024		
13,171	4,12	4,121	0,024		
12,928	4,05	4,053	0,074		
12,344	3,875	3,877	0,052		
11,788	3,703	3,706	0,081		
11,233	3,531	3,53	0,028		
10,527	3,311	3,311	0,000		
		Average:	0,077		
		Median:	0,040		

Figure 32: Verification of DPL Circuit

High Current Circuit			
U_Voltage Source	U_VM node 1 [V]	U_Arduino_node1 [V]	Error node1 [%]
14	2,99	2,983	0,007
13,7	2,98	2,979	0,001
13	2,98	2,974	0,006
12,302	2,98	2,974	0,006
11,401	2,98	2,974	0,006
10,2	2,98	2,974	0,006
8,2	2,54	2,539	0,001
7,2	2,23	2,231	0,001
6,5	2,02	2,012	0,008
5,7	1,77	1,763	0,007
		Average:	0,0049
		Median:	0,006

Figure 33: Verification of High Current Circuit

A.4 Verify Capacity Measurement Board

Capacity Measurement Board Pos 1-6													
Position 1				Position 2				Position 3					
U_VS	U_calculated [V]	Error [mV]	Error [%]	U_VS	U_calculated [V]	Error [mV]	Error [%]	U_VS	U_calculated [V]	Error [mV]	Error [%]		
14,5	14,50614489	6,14488769	0,04237854	14,5	14,50513284	5,13284149	0,03539891	14,5	14,50664932	6,64932166	0,04586		
14	14,00233866	2,33865805	0,0167047	14	14,00256551	2,56551484	0,01832511	14	14,00402945	4,02945269	0,02878		
13,8	13,79386711	6,13288524	0,0444412	13,8	13,79460662	5,39337894	0,03908246	13,8	13,79604882	3,95118275	0,02863		
13,5	13,49853243	1,46757158	0,0108709	13,5	13,4999819	0,0018118	1,3421E-05	13,5	13,50140958	1,40958372	0,01044		
13	12,9947262	5,27380121	0,0405677	13	12,99743086	2,56913845	0,0197626	13,5	13,50140958	1,40958372	0,01044		
12,5	12,49091997	9,08003084	0,07264025	12,5	12,49486353	5,1364651	0,04109172	13	12,99878971	1,21028525	0,00931		
12	12,00448637	4,48636813	0,0373864	12	11,99229621	7,70379174	0,06419826	12,5	12,49616985	3,83015422	0,03064		
11,5	11,50068014	0,6801385	0,00591425	11,5	11,50750879	7,05878942	0,06138078	12	11,99354998	6,45002319	0,05375		
11	10,99687391	3,12609113	0,02841901	11	11,00494146	4,49146278	0,04083148	11,5	11,49093011	9,06989216	0,07887		
10,5	10,49306768	6,93232076	0,0660221	10,5	10,50192414	1,92413613	0,01832511	11	11,00564196	5,64195849	0,05129		
10	9,98926145	10,7385504	0,1073855	10	9,999356809	0,64319051	0,00643191	10,5	10,50302209	3,02208952	0,02878		
9,5	9,502827849	2,82784858	0,02976683	9,5	9,496789483	3,21051716	0,03379492	10	10,00040222	4,40222055	0,00402		
9	8,999021619	0,97838105	0,0108709	9	8,994222156	5,77784381	0,06419826	9,5	9,497782352	2,21764842	0,02334		
	Average	4,63134871	0,03948987		Average	3,96991401	0,03406423	9	8,995162483	4,83751739	0,05375		
	Median	4,48636813	0,0373864		Median	4,49146278	0,03539891		Average	4,05548692	0,03442		
									Median	3,95118275	0,02878		
Position 4				Position 5				Position 6					
U_VS	U_calculated [V]	Error [mV]	Error [%]	U_VS	U_calculated [V]	Error [mV]	Error [%]	U_VS	U_calculated [V]	Error [mV]	Error [%]		
14,5	14,5031467	3,14670139	0,02170139	14,5	14,50700419	7,00418558	0,04830473	14,5	14,50700419	7,00418558	0,0483		
14	14,00124783	1,24782986	0,00891307	14	14,00497182	4,97182116	0,03551301	14	14,00497182	4,97182116	0,03551		
13,8	13,8108724	10,8723958	0,07878548	13,8	13,81454575	14,5457519	0,105404	13,8	13,79723429	2,76570894	0,02004		
13,5	13,49934896	0,65104167	0,00482253	13,5	13,50293946	2,93945674	0,02177375	13,5	13,50293946	2,93945674	0,02177		
13	12,99745009	2,54991319	0,01961472	13	13,00090709	0,90709233	0,00697763	13	13,00090709	0,90709233	0,00698		
12,5	12,49555122	4,44878472	0,03559028	12,5	12,49887473	1,12527209	0,00900218	12,5	12,49887473	1,12527209	0,009		
12	11,99365234	6,34765625	0,05289714	12	11,99684236	3,15763651	0,02631364	12	11,99684236	3,15763651	0,02631		
11,5	11,50906033	9,06032986	0,07878548	11,5	11,49481	5,19000093	0,04513044	11,5	11,49481	5,19000093	0,04513		
11	11,00716146	7,16145833	0,06510417	11	10,99277763	7,22236534	0,06565787	11	10,99277763	7,22236534	0,06566		
10,5	10,50526259	5,26258681	0,05011987	10,5	10,49074527	9,25472976	0,08814028	10,5	10,50805673	8,05673108	0,07673		
10	10,00336372	3,36371528	0,03363715	10	10,00602437	6,02436666	0,06024367	10	10,00602437	6,02436666	0,06024		
9,5	9,501464844	1,46484375	0,01541941	9,5	9,503992002	3,99200225	0,04202108	9,5	9,503992002	3,99200225	0,04202		
9	8,999565972	0,43402778	0,00482253	9	9,001959638	1,95963783	0,02177375	9	9,001959638	1,95963783	0,02177		
	Average	4,30856036	0,03617025		Average	5,25340916	0,04432739		Average	4,25509826	0,03688		
	Median	3,36371528	0,03363715		Median	4,97182116	0,04202108		Median	3,99200225	0,03551		

Figure 36: Verification of Capacity Measurement Board Position 1-6

Capacity Measurement Board Pos 7-10												
Position 7				Position 8				Position 9				
U_VS	U_calculated [V]	Error [mV]	Error [%]	U_VS	U_calculated [V]	Error [mV]	Error [%]	U_VS	U_calculated [V]	Error [mV]	Error [%]	
14,5	14,50700419	7,00418558	0,04830473	14,5	14,5090107	9,01069627	0,06214273	14,5	14,50299465	2,99464651	0,02065	
14	14,00497182	4,97182116	0,03551301	14	14,00750735	7,50734682	0,05362391	14	14,00110104	1,10103702	0,00786	
13,8	13,81454575	14,5457519	0,105404	13,8	13,79998872	0,01128054	8,1743E-05	13,8	13,79342092	6,57907725	0,04767	
13,5	13,50293946	2,93945674	0,02177375	13,5	13,506004	6,00399736	0,04447405	13,5	13,49920743	0,79257246	0,00587	
13	13,00090709	0,90709233	0,00697763	13	13,00450065	4,50064791	0,03462037	13	12,99731382	2,68618195	0,02066	
12,5	12,49887473	1,12527209	0,00900218	12,5	12,5029973	2,99729845	0,02397839	12,5	12,49542021	4,57979143	0,03664	
12	11,99684236	3,15763651	0,02631364	12	12,00149395	1,493949	0,01244958	12	11,9935266	6,47340092	0,05395	
11,5	11,49481	5,19000093	0,04513044	11,5	11,4999906	0,00940045	8,1743E-05	11,5	11,49163299	8,36701041	0,07276	
11	10,99277763	7,22236534	0,06565787	11	10,99848725	1,51274991	0,01375227	11	10,98973938	10,2606199	0,09328	
10,5	10,49074527	9,25472976	0,08814028	10,5	10,4969839	3,01609936	0,02872476	10,5	10,50515245	5,15244681	0,04907	
10	10,00602437	6,02436666	0,06024367	10	9,995480551	4,51944882	0,04519449	10	10,00325884	3,25883733	0,03259	
9,5	9,503992002	3,99200225	0,04202108	9,5	9,493977202	6,02279827	0,06399788	9,5	9,501365228	1,36522784	0,01437	
9	9,001959638	1,95963783	0,02177375	9	8,992473852	7,52614772	0,08362386	9	8,999471618	0,52838164	0,00587	
Average	5,25340916	0,04432739		Average	4,1639893	0,03585737		Average	4,16455627	0,03548		
Median	4,97182116	0,04202108		Median	4,50064791	0,03462037		Median	3,25883733	0,03259		
Position 10												
U_VS	U_calculated [V]	Error [mV]	Error [%]									
14,5	14,50343266	3,43265526	0,02367348									
14	14,00212211	2,12211056	0,01515793									
13,8	13,79468326	5,31673552	0,03852707									
13,5	13,50081157	0,81156587	0,0060116									
13	12,99950102	0,49897883	0,0038383									
12,5	12,49819048	1,80952353	0,01447619									
12	11,99687993	3,12006823	0,02600057									
11,5	11,49556939	4,43061293	0,03852707									
11	10,99425884	5,74115763	0,05219234									
10,5	10,4929483	7,05170233	0,06715907									
10	9,991637753	8,36224703	0,08362247									
9,5	9,490327208	9,67279173	0,10181886									
9	8,989016664	10,9833364	0,12203707									
Average	4,87334507	0,04561862										
Median	4,43061293	0,03852707										

Figure 37: Verification of Capacity Measurement Board Position 7-10

A.5 Self discharge curves for all batteries

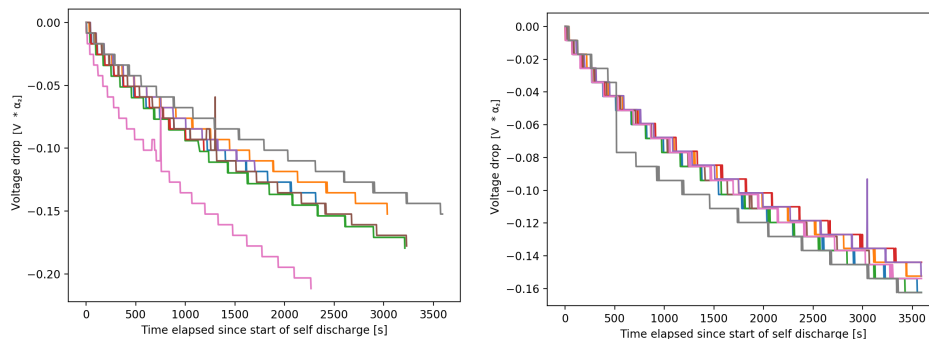


Figure 38: Self discharge curves.

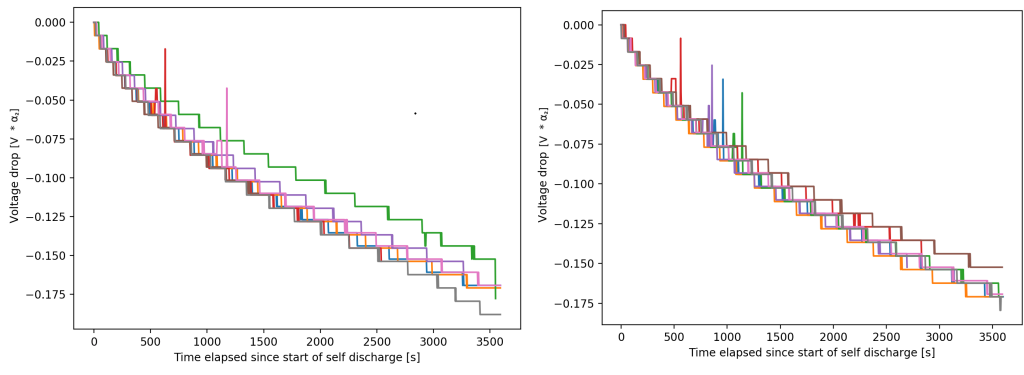


Figure 39: Self discharge curves.

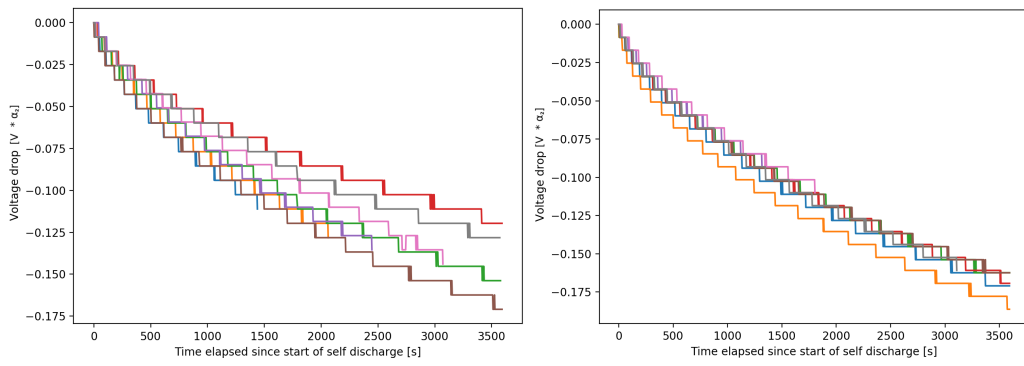


Figure 40: Slow discharge curves.

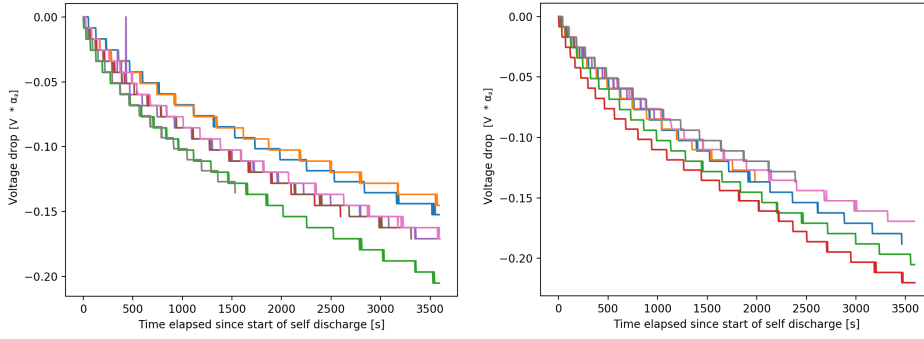


Figure 41: Slow discharge curves.

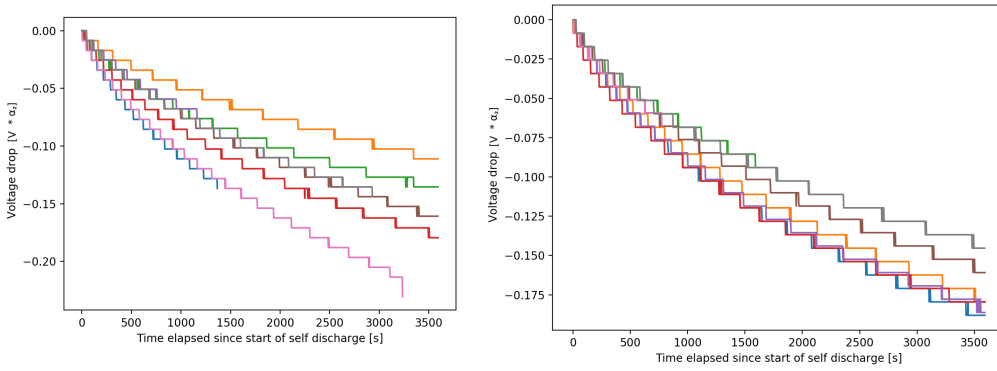


Figure 42: Slow discharge curves.